Summer 8-2011

Effects of oxidative stress on cultured spermatogenic cycts and an ultrastructural analysis of the testes in Drosophila pseudoobscura
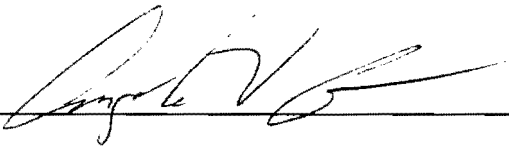
Robert W. Yates
Seton Hall University

Effects of oxidative stress on cultured spermatogenic cysts and an ultrastructural analysis of the testes in *Drosophila pseudoobscura*

Robert W. Yates

Submitted in partial fulfillment of the requirements for the Degree of Master of Science
in Biology from the Department of Biological Sciences of Seton Hall University
August 2011

APPROVED BY

_____

MENTOR

Dr. Angela V. Klaus

_____

COMMITTEE MEMBER

Dr. Allan Blake

_____

COMMITTEE MEMBER

Dr. Tin-Chun Chu

_____

DIRECTOR OF GRADUATE STUDIES

Dr. Allan Blake

_____

CHAIRPERSON, DEPARTMENT OF BIOLOGICAL SCIENCES

Dr. Jane Ko

ACKNOWLEDGEMENTS

TABLE OF CONTENTS

LIST OF FIGURES

LIST OF TABLES

Effects of oxidative stress on cultured spermatogenic cysts and an ultrastructural analysis of the testes in *Drosophila pseudoobscura*

Robert W. Yates

Submitted in partial fulfillment of the requirements for the Degree of Master of Science
in Biology from the Department of Biological Sciences of Seton Hall University
August 2011

Abstract

Spermatogenesis is a series of processes that lead to the development of haploid mature sperm from diploid stem cells. Cellular glutathoine (GSH) is a known antioxidant and reducing agent against reactive oxygen species. Recent evidence from our laboratory suggests that the survivability of *Drosophilia pseudoobscura* fly spermatogenic cysts in *in vitro* culture can be improved by adding exogenous GSH to the culture media. Pupal cysts are ideal for cyst cultures due to their increased numbers of early-stage cysts compared to sexually-active adult flies. This allows for better quantification of their survivability. In the current work, the effect that diminished endogenous GSH expression would have on spermatogenic cyst survival *in vitro* was studied. Buthionine sulfoximine (BSO) is a known inhibitor of intracellular GSH production. By adding BSO to *D. pseudoobscura* spermatogenic cyst cultures, and measuring the survivability of different cyst types over 96 hours, we determined that early spermatogenic cysts (spermatogonia and primary spermatocytes) are extremely susceptible to degradation due to oxidative stress. Results show that 0-24 hour cysts are little affected by oxidative stress; however, by 48 hours, there was a large increase in cellular degradation and debris as well as abnormalities in cyst development in comparison to controls. Additionally, in later cultures, it was noted that many of the elongating cysts were susceptible to degradation due to oxidative stress. Cyst abnormalities ranged from incomplete and uneven elongation to uneven cell proliferation and growth resulting in unusual cyst morphologies. Furthermore, Hoechst stains of BSO-treated cultures suggest the abnormal elongation to be a failure of a cyst cell to correctly initiate elongation.

Introduction

I. Overview

Spermatogenesis is a complex and regulated process that results in the differentiation and transformation of germline stem cells into mature and motile spermatozoa that are able to deliver the paternal genetic material successfully to the maternal egg. The process of spermatogenesis involves the mitotic expansion of one germline stem cell, meiosis, and a post-meiotic process called spermiogenesis. Spermiogenesis includes nuclear condensation and transformation, the biogenesis of the acrosome, the reorganization of and relocation of the mitochondria to the sperm mid-piece, growth of the flagellum necessary for motility, and the removal of the vast majority of the cytoplasm and cellular machinery (Cheng and Mruk 2011). Spermatogenesis occurs in species spanning the animal kingdoms and although there are differences, similarities between spermatogenesis in different organisms has led to the acceptance of several organisms as "model" organisms for the experiments within that discipline (Lo 2011). *Drosophila melanogaster* has been a model organism since its initial use in genetic experiments in the 1960's, and has become an important organism in spermatogenesis research (Cross and Shellenbarger 1979).

II. Spermatogenesis and *Drosophila melanogaster* as a Model Organism

Spermatogenesis involves the transformation of a single diploid stem cell into multiple haploid cells, followed by their transformation from round cells into mature and motile spermatozoa. Several organisms, such as *C. elegans* and *D. melanogaster*, are

being used as "models" to mimic human processes for experiments in developmental and cellular biology. *Drosophila* is a genus in the Drosophilidae family of the kingdom Animalia containing most notably the *melanogaster* subgroup. *Drosophila* is commonly used in genetic research because the genomes of the three species in the *melanogaster* subgroup, along with the 9 other other *Drosophila* species, have been sequenced (Markow 2007). *D. melanogaster*'s easy care, high reproductive and offspring survivability rates, as well as their susceptibility to genetic manipulation, make it an excellent organism with which to experiment in cases where utilizing humans or mammals would be inappropriate (White-Cooper 2008).

Spermatogenesis in *D. melanogaster* occurs much in the same way as in mammals; however, with some important differences. In mammalian and fly spermatogenesis, the daughter cell of one germline stem cell goes through a mitotic expansion and two meiotic divisions, then differentiates into mature spermatozoa (Fuller 1998). In mammals, this transformation is aided by the Sertoli cells, a specific type of somatic cell which functions to form the blood-testis barrier, and support the meiotic and transforming cells with nutrients (Phillips *et. al.* 2010). During the post-meiotic transformation (called spermiogenesis), the spermatozoan nucleus goes through dramatic changes in structure and form, including the development of the acrosome, the rearrangement of the mitochondria, and the growth of the flagellum utilized in propelling the sperm. *D. melanogaster* mimics the nuclear transformation process, although not into the same shape, the biogenesis of the acrosome, and other main structural changes; however, *D. melanogaster* does have many differences when compared to mammals.

3

D. *melanogaster* testes are blind tubes with an apical end, where the germline

stem cell "niche" is located, and a basal end, where the testes connect to the seminal

vesicles (Fuller 1998). Its germline stem cells are not organized in the same manner as in

mammals. In contrast to a basal layer of germline stem cells, the germline stem cells are

attached to a group of somatic cells, or hub cells, in a "rosette" fashion (Hardy 1979). It is

the interaction between these hub cells and the germline stem cells that allows them to

maintain their function and not differentiate into somatic cells. Also within the stem cell

niche are cyst progenitor cells, aligned adjacent to each germline stem cell, which divide

as the stem cell divides. Two cyst cells per germline cell divide providing "head" and

"tail" cells to encapsulate the newly-dividing spermatogonia. The result of a germline

stem cell division is a daughter cell flanked by cyst progenitor cells still attached to the

hub of somatic cells, as well as a daughter cell surrounded by cyst cells detached from the

hub. In *D. melanogaster*, the detached daughter cell goes through four mitotic divisions

before entering meiosis and spermatogenesis. The arrangement of hub cells, cyst

progenitor cells, and germline cells is shown in Figure 1C.

Ultimately, spermatogenesis in *D. melanogaster* results in 64 mature and motile

sperm. Following the end of meiosis, however, the 64 haploid spermatids are round cells

connected through cytoplasmic bridges to each other. The round spermatids enter an

elongation process where the tails grow and the heads begin transformation. Once

elongation is completed, the now-elongated spermatids go through a process called

individualization where a plasma membrane is deposited around each individual

spermatid, thus removing the majority of the excess cytoplasm in the process. A cystic

bulge structure marks the individualization process. The now-individualized sperm are still encapsulated in the two cyst cells, and the excess cytoplasm is discarded as a waste bag (Tokuyasu 1972).

Once the cysts have migrated into the basal end of the testis, they embed into the basal epithelium giving the spermatozoan the mechanical anchor to coil up the tail in order to compact the sperm for storage in the seminal vesicles. It is thought that along with mechanical aid, the epithelial cells may be providing a substance which aids in the degeneration of the cyst cells releasing the sperm cells to enter the seminal vesicles for storage before ejaculation (Njogu *et. al.* 2010). It is unknown whether there is an interaction between the sperm and this epithelial layer that either aids in or is necessary for motility and correct coiling of mature spermatozoa. Although there are many differences between humans and *D. melanogaster* in spermatogenesis, the mechanics of many of the processes are similar. It is these similarities, as well as some of the differences, that make *Drosophila* a useful model for spermatogenesis research. Many of the spermatogenic steps are conserved between *D. melanogaster* and humans. A visual representation of *D. pseudoobscura* spermatogenesis can be seen in Figure 1.
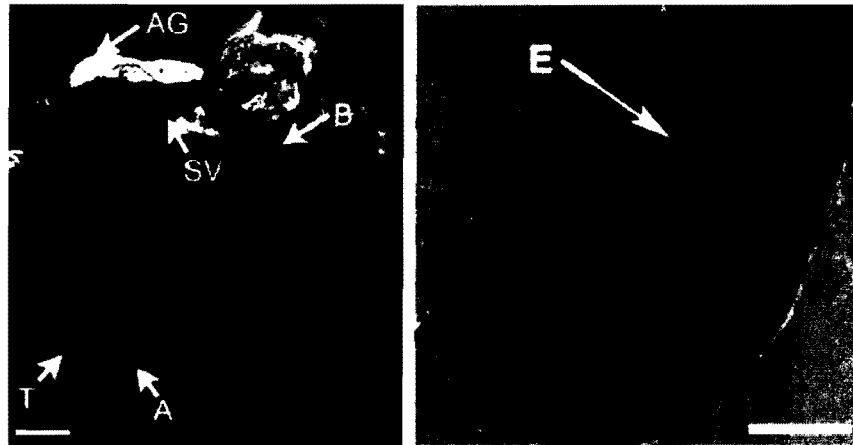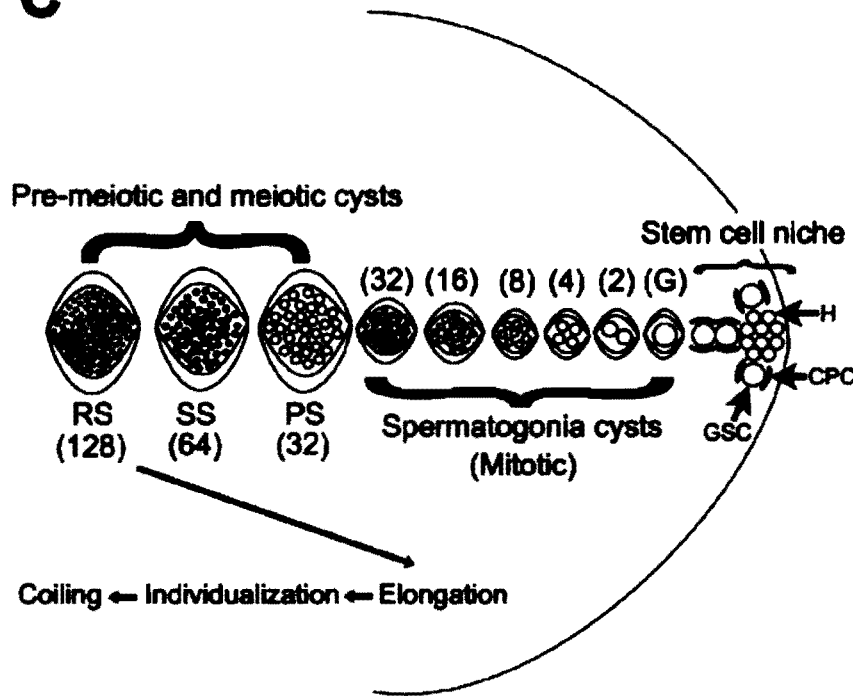
Figure 1: A. Paired *D. pseudoobscura* testes (T), seminal vesicles (SV), and accessory glands (AG). The stem cell niche, as indicated in panel C, is located in the apex (A). Sperm coiling occurs in the basal end (B) and coiled sperm are stored in the SV. B. Single testis (E) indicating elongating cysts spanning almost the entire length of the testis. Phase contrast and brightfield. Scale bars = 100 μm. (As adapted from Ricketts *et. al.* 2011)

Although the model organism of this genus is *D. melanogaster*, the utilization of *D. pseudoobscura*, another species in the genus *Drosophila*, for spermatogenesis experiments rather than *D. melanogaster* has distinct advantages. *D. melanogaster* spermatozoa have been shown to grow to a retarded length of 500 microns *in vitro*, in comparison to 1800 microns *in vivo* (Cross and Shellenbarger 1979). Mature *D. pseudoobscura* have a shorter spermatozoan length of about 400 microns *in vivo* and *in vitro*. According to Njogu *et. al.* (2010), *D. pseudoobscura* cysts are more viable in culture. The ellipsoid morphology of *D. pseudoobscura* testes allows for easier detection and makes them much easier to work with compared to the highly coiled and fragile *D. melanogaster* testes. Due to these unique features, its sequenced genome, and close evolutionarily relationship with *D. melanogaster*, *D. pseudoobscura* has been used for studies of spermatogenesis (Njogu *et. al.* 2010).

III. Ultrastructure of *Drosophila* Testes

D. melanogaster* has, as previously mentioned, a highly coiled and fairly fragile testis. The ultrastructure of *D. melanogaster* is well known (Tokuyasu 1972, 1974), as well as the nuclear organizational details that occur during nuclear transformation (Tokuyasu 1975). The structure of a *D. melanogaster* testis is very different from *D. pseudoobscura*. The ellipsoid nature of the *D. pseudoobscura* testis is similar to that of the structure in the Mexican fruit fly of the Diptera family. Transmission electron microscopy data of this fly, *Anastrepha ludens*, whose testis morphology is very similar to the *D. pseudoobscura* testes, is available (Valdez 2001).

A well-developed layer of smooth muscle is present between the interior and

exterior epithelium of *Anastrepha ludens* (Valdez 2001).Valdez postulates that the smooth muscle in the wall of the *A. ludens* testis functions to aid in the movement of developing cysts from the blind apical end to the basal end of the testis. The highly coiled and narrow testis of *D. melanogaster* allows for the movement of the developing cysts from the apical end to the basal end via pressure of new cysts from the apical end. Due to the ellipsoid nature of the *D. pseudoobscura* testis, a muscle layer similar to that found in *A. ludens* may be present.
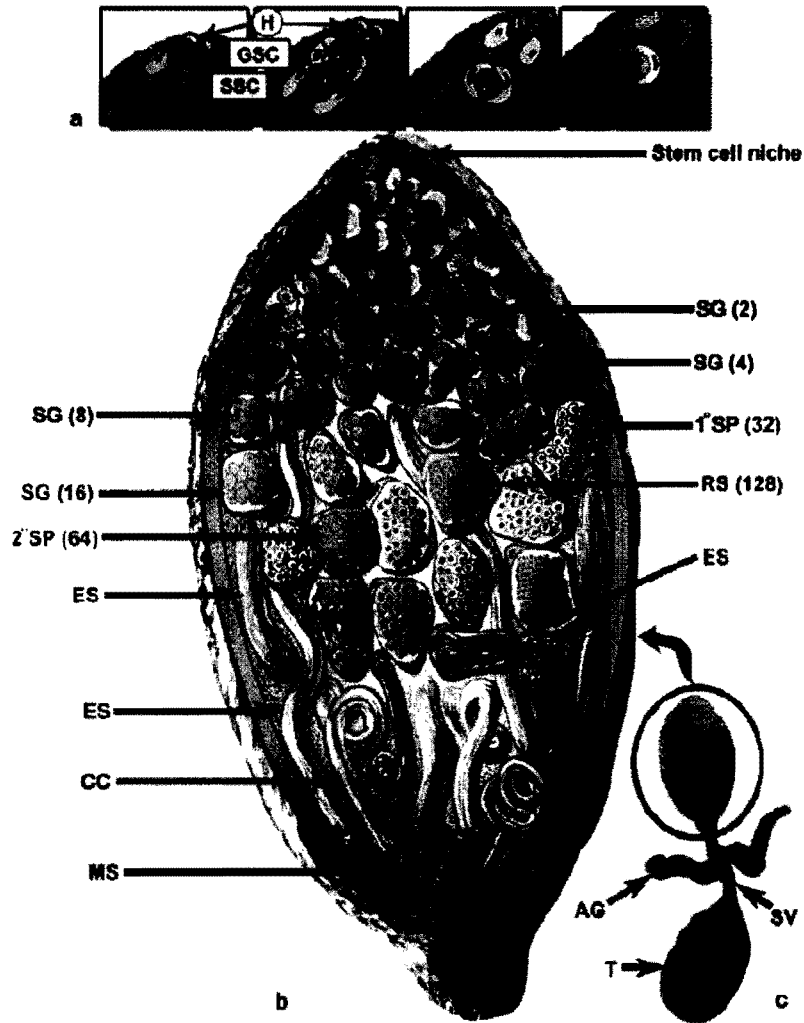
Figure 2: An illustration of spermatogenic cyst maturation in *D. pseudoobscura*. The stem cell niche and the division of germ line stem cells and cyst cells are show in A. B shows the progression of cysts through spermatogenesis. The stages of the cysts are indicated next to the arrows with the number of spermatogenic cells indicated in parentheses. The pair of testes is depicted in C. T=Testis, SV=Seminal Vesicle, AG=Accessory Gland. (As adapted from Njogu *et. al.* 2010).

IV. Glutathione and Buthionine Sulfoximine

Glutathoine (GSH) is a small tripeptide, γ-L-glutamylcysteinylglycine, which serves several physiological functions. GSH has three main cellular functions. First is the maintenance of cellularly-important thiols, such as on proteins, antioxidants and other compounds. Second is the reduction of ribonucleotides to form the deoxyribonucleotide molecules found in DNA. Lastly, GSH functions as protection against oxygen-free radicals which have highly-reactive free electrons responsible for cytotoxicity (Rebrin and Sohal 2009). GSH is intracellularly synthesized in the cytoplasm of cells via two sequential ATP-dependent enzymes: γ –glutamylcysteine synthetase and glutathione synthetase (Rebrin and Sohal 2009). GSH is a versatile reducing agent; therefore, it can act as an antioxidant and quench radicals, provide reducing equivalents for enzymes, maintain protein thiol groups, and act as a coenzyme, along with others (Rebrin and Sohal 2009).

GSH is intracellularly compartmentalized with concentration differences, creating micro-redox environments in each compartment. For example, it is known that GSH is normally low in the nucleus and higher in the cytoplasm, and is recruited into the nucleus during cell proliferation (Borras *et. al.* 2007). The main importance of GSH in the cell is its function as a reducing agent or an antioxidant against mainly hydrogen peroxide and lipid peroxides (Krzywanski *et. al.* 2004). In insects, the GSH and thioredoxin reduction systems, two important reducing systems in the cell, are major antioxidant systems for the removal of reactive oxygen species (ROS) (Missirlis 2001). Evidence indicates that the survivability of *D. pseudoobscura* fly sperm cyst cells can be increased by adding

exogenous GSH to the culture media when compared to a control (Ricketts *et. al.* 2011 ; Nikki *et. al.* 2006); however, it still remains to be seen what effect cellularly-produced GSH has on the survivability of cells, and to what degree.

Buthionine sulfoximine (BSO) is a known inhibitor of intracellular GSH production (Meister 1991). BSO effectively binds to and inactivates γ –glutamylcysteine synthetase, the rate limiting enzyme in the GSH synthesis pathway. It is specifically used to inhibit GSH production because it is specific in its binding and does not also inhibit glutamine synthetase. Adding BSO to culture systems effectively shuts off GSH production by the cells (Meister 1991; Anderson 1998). Having no functional GSH removes one of the cells most valuable antioxidant systems resulting in the increase of ROS and oxidative stress (Missirlis *et al.* 2001). This system is present in *Drosophila* (Kanzok *et. al.* 2001), and BSO has been shown to be effective for producing oxidative stress conditions in cultured *Drosophila* cells (Missirlis *et. al.* 2001). The regeneration of oxidized GSH to the active, reduced form that occurs via the glutathione reductase pathway or a thioredoxin system (Anderson 1998) is well-characterized, with the latter existing in *D. melanogaster* (Blokhina *et. al.* 2003, Allocati *et. al.* 2009).

V. Current Approach

The purpose of the current work was to explore the effect of intracellularly-produced GSH on spermatogenic cyst degeneration, specifically early spermatogonial cysts which are more susceptible than other cyst types to oxidative stress. This differs from previous experiments done in the lab that were focused on the effect of exogenous GSH. Using BSO in culture disrupts the enzyme, γ –glutamylcysteine synthetase, by

11

binding to the active site. This inhibits the enzyme responsible for cellular production of

γ –glutamylcysteine, one of the substrates for GSH synthetase (Meister 1991, Anderson

1998).

To test our hypothesis that the GSH production system will be disrupted in

cultured *D. pseudoobscura* spermatogenic cysts, we measured the survivability of the

different cyst types in 96-hour BSO-treated cultures. We hypothesized that cultures

without cellularly-produced GSH would show more degradation of cysts as compared to

controls. By comparing overall cyst percentages and cyst degeneration rates, we show

that intracellular GSH is needed for the survival of early spermatogenic cysts, primary

spermatocytes especially, and for the proper organization of elongating cysts.

Additionally, we were interested in investigating the ultrastructure of the *D.*

pseudoobscura testis wall and the association of elongated spermatogenic cysts with the

basal epithelium. Previous work in our lab suggested that cyst coiling and motility may

be affected by such an association (Njogu *et. al.* 2010).

Materials and Methods

I. Fly Stock

Fly stocks were obtained from the University of California San Diego *Drosophila* Species Stock Center. All flies were cultured at 25°C in our laboratory on Jazz Mix (Fisher Scientific 2011) *Drosophila* medium.

II. Culture Medium

The culture medium was based on a previous study by Cross and Shellenbarger (1979) as modified from Cross and Sang (1978). Shields and Sang M3 Powdered insect media without bicarbonate (Sigma-Aldrich) was rehydrated following the manufacturer's instructions. The M3 insect media was supplemented with 10% heat-inactivated fetal calf serum (Sigma-Aldrich). The media was further supplemented with 1% penicillin/streptomycin according to previous studies (Njogu *et. al.* 2010, Niki *et. al.* 2006, Kawamoto *et. al.* 2008). For the *in vitro* experiments with isolated cysts, BSO was added to the M3 medium at a concentration of 1 mM. The concentration of BSO was determined from previous studies involving neurons (Liebmann *et. al.* 1993, Anderson and Reynolds 2002, Blake 2004). Culture medium for control cultures was as described above, without BSO, and supplemented with 0.6 mg/ml of GSH.

III. Testes Dissection and Cyst Isolation

Five to seven day old pupae were selected for culture, isolated, and soaked in 70% ethanol for ten minutes prior to dissection. Dark-bodied pupae with healthy, bright-red testes were selected for culture. The dissection tools and depression slides were sterilized

13

with 70% ethanol before and during use. The pupae were removed from the pupal case, decapitated, and the testes were removed. The pupae were dissected on a shallow depression slide in M3 media prepared as described above. The testes were removed and placed in M3 medium while further dissections were completed. To release the cysts, the testes were held near the basal end and torn near the apical end in order to release the maximum amount of cysts. Cysts from three pairs of testes were used for each culture well. After the testes tissue was removed and the cysts were pushed towards the center of the slide depression, the slide was transported to a sterile laminar flow hood. Using a pipet with a portion of the selected volume already drawn, the cysts were extracted from the well until the remaining portion of the selected volume was filled. Using the technique described above, all of the extracted cysts and a total of 1 ml of prepared media were deposited into a well on a 24-well culture plate. The culture was left to sit in the hood allowing time for the cysts to settle, then the plate was tapped to disperse the cysts throughout the well for initial counting.

IV. *In vitro* BSO Cyst Culture

The testes were dissected as described above and then teased open using dissection tools to spill out the cysts. The cysts often stay in a mass which resemble the shape of the testes. They were transported via pipetman into 50 µL of prepared media on a sterilized depression slide. The media was prepared as above with 100 µL of 0.055 g/mL of BSO, to make a final concentration of 1 mM. The media was added to a 24-well culture plate with a 1 mm x 1 mm grid drawn on the bottom of the well in ultrafine red marker. The cysts in the 50 µL of media were transported to the hood where the contents

14

of three pairs of testes were added into 1000 µL of prepared media per well and cultured
for 96 hours.

V. Quantification of Cultured Cysts and Statistics

The BSO and control cyst cultures were maintained for five days with viable cysts

counted every 24 hours, starting at 0 hour and ending at 96 hours. The cysts were

categorized according to type: 8-32 cell spermatogonia, 32 cell primary spermatocytes,

64 cell secondary spermatocytes, and 128 cell round spermatid cysts. Cysts were

considered viable if the cyst cells were intact, and there was no indication of either cyst

cell or spermatogenic cell degeneration. Abnormal cysts were counted if they were

viable. Elongating cysts in large bunches were not counted as it is difficult to differentiate

them from one another. The cysts were counted accurately by using a 1 mm x 1 mm grid

system as previously described. The initial square of the grid counted was the top left

square. Counting progressed horizontally from the first square of each row to the last

while moving down in a zigzag pattern reversing the counting direction for each

subsequent row. Any cysts within the edges of the four grid lines or inside of the left and

bottom grid lines were counted for that particular square on the grid. The cysts were

counted on an inverted phase contrast Leica DMIL microscope. Statistics were computed

using Graphpad Prism.

VI. Transmission Election Microscopy

Transmission electron microscopy was done on whole, paired testes using pupal

flies dissected as described above. The testes were fixed in 2.5% glutaldehyde in 0.1 M

phosphate buffer (pH 7.2) for two hours at room temperature. The glutaldehyde was

removed using a glass Pasteur pipet and the testes were then rinsed three times in 0.1 M

phosphate buffer (pH 7.2) for 10 minutes each rinse. The testes were post-fixed with 1%

osmium tetroxide/0.1 M phosphate buffer. The second fixation was done in the fume

hood for two hours. The osmium tetroxide was removed and the testes were rinsed three

times with 0.1 M phosphate buffer for 10 minutes each rinse.

After the final rinse, the testes were dehydrated with 15-minute soaks in

increasing concentrations of ethanol at 50%, 70%, and 95%, and two 20-minute soaks in

100% ethanol. Following dehydration, the testes were placed in 100% acetone for 15

minutes. Two one-hour soaks in 1:1 acetone:embedding medium (Embed 812, Electron

Microscopy Sciences) were followed by an overnight infiltration in 1:2

acetone:embedding medium. The following day, the 1:2 solution was replaced with 100%

resin. The testes were infiltrated with two changes of 100% resin over the course of 2 -6

hours. The samples were then placed at the bottom of plastic BEEM capsules (Electron

Microscopy Sciences) and the capsules were filled with 100% resin. The capsules were

placed in a 60°C oven overnight to polymerize the resin mounts.

The specimens were removed from the capsules using a specialized press. An

ultramicrotome equipped with a diamond knife was used to section the embedded testes

into ultrathin sections, approximately 80 nm in thickness. Sections were picked up on 200

mesh copper grids, stained in uranyl acetate for 45 minutes, and thoroughly rinsed in

deionized water. The sections were viewed on a FEI Tecnai G2 Spirit Transmission

Electron Microscope.

VII. Confocal Microscopy

Hoechst 33342 (Sigma-Aldrich) was added to the culture well with a final concentration of 0.5 µg/ml. The cysts were initially viewed on an inverted phase contrast Leica DMIL microscope to confirm successful staining. Cysts were gently removed with a pipet from the culture plate in 300 µl increments and moved into the well on a cover slip for high resolution imaging. Three wells on a cover slip were prepared and they were imaged on an Olympus FV1000 confocal laser scanning microscope.

Results

I. Cyst Quantification and Statistics

Cyst quantification was completed over the course of 96 hours. The cysts were grouped as follows: 8-32 cell spermatogonia (SG), 32 cell primary spermatocytes (PS), 64 secondary spermatocytes + 128 cell round spermatids, elongating, and coiling cysts, as shown in Figure 3. Secondary spermatocytes and round spermatids were counted as one group as it was difficult to distinguish between them due to very similar morphology. The cells were counted every 24 hours at the same time everyday throughout the 96-hour experimental period. Counting took approximately one hour per well; quantification was completed as quickly as possible in order to minimize light exposure to the cysts. Statistics were completed on average cyst percentages using Microsoft Excel and Graphpad Prism statistical software. Two-tailed t-tests were used in determining significant differences and in constructing graphs. A total of three experiments were performed for the BSO trial and a total of four experiments were done for the control.
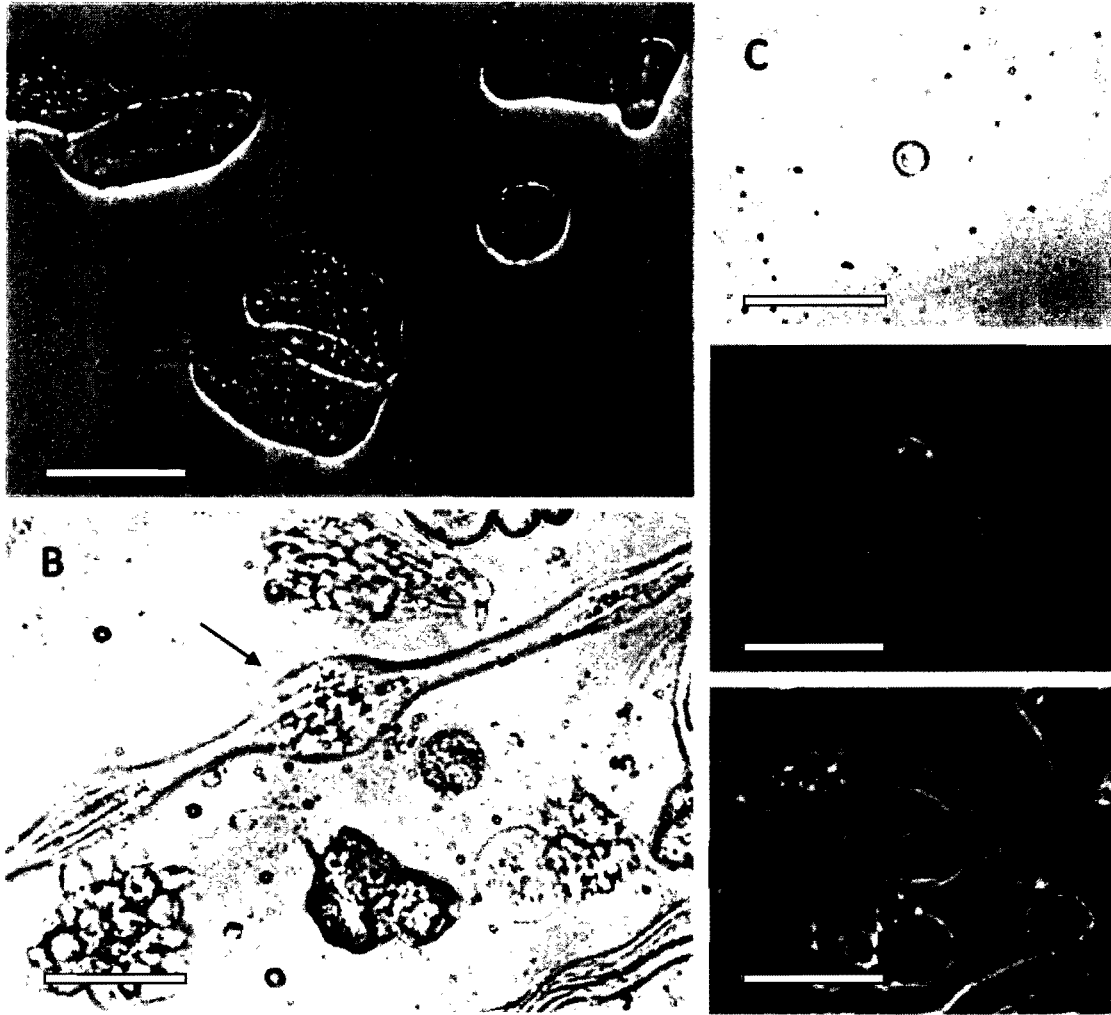
Figure 3: Examples of cyst quantification categories. Brightfield images at 400X. (A) From top right – elongating cyst, 16 cell spermatogonia (SG), secondary spermatocyte/round spermatids. (B) Individualizing cyst. (C) 8 cell SG. (D) Primary spermatocyte (PS). (E) Coiling cyst. Scale Bars = 100 μm.

BSO Trial 1	0 hr	24 hr	48 hr	72 hr	96 hr
Spermatogonia	119	103	23	5	5
Primary Spermatocytes	92	17	0	0	0
Secondary Spermatocytes + Round Spermatids	72	118	107	93	89
Elongating Cysts	459	259	163	116	101
Coiling Cysts	0	77	50	41	54
Total Cyst Number	742	574	343	255	249

BSO Trial 2	0 hr	24 hr	48 hr	72 hr	96 hr
Spermatogonia	108	84	28	8	6
Primary Spermatocytes	127	25	2	0	0
Secondary Spermatocytes + Round Spermatids	86	117	73	68	66
Elongating Cysts	488	492	336	296	252
Coiling Cysts	0	42	52	41	38
Total Cyst Number	809	760	491	414	362

BSO Trial 3	0 hr	24 hr	48 hr	72 hr	96 hr
Spermatogonia	170	135	66	32	20
Primary Spermatocytes	122	39	2	0	0
Secondary Spermatocytes + Round Spermatids	148	94	72	66	51
Elongating Cysts	852	773	761	603	541
Coiling Cysts	0	134	159	107	86
Total Cyst Number	1292	1175	1060	808	698

Table 1: Quantification of viable cysts at different stages in cultures treated with BSO at a concentration of 1 mM.

Control Trial 1					
	0 hr	24 hr	48 hr	72 hr	96 hr
Spermatogonia	123	99	88	83	73
Primary Spermatocytes	87	71	55	41	28
Secondary Spermatocytes + Round Spermatids	81	62	67	58	39
Elongating Cysts	735	784	803	816	701
Coiling Cysts	0	38	47	40	39
Total Cyst Number	1026	1054	1060	1038	880

Control Trial 2					
	0 hr	24 hr	48 hr	72 hr	96 hr
Spermatogonia	142	112	94	78	56
Primary Spermatocytes	96	59	42	33	17
Secondary Spermatocytes + Round Spermatids	86	60	66	47	44
Elongating Cysts	589	632	601	519	565
Coiling Cysts	0	68	111	117	205
Total Cyst Number	913	931	914	794	887

Table 2: Quantification of viable different stage cysts in cultures treated with GSH at a concentration of 0.6 mg/ml, for cultures 1 and 2.

Control Trial 3					
	0 hr	24 hr	48 hr	72 hr	96 hr
Spermatogonia	136	108	77	66	60
Primary Spermatocytes	103	89	66	51	22
Secondary Spermatocytes + Round Spermatids	101	99	72	55	54
Elongating Cysts	605	534	533	466	412
Coiling Cysts	0	56	121	118	102
Total Cyst Number	945	886	869	756	650

Control Trial 4					
	0 hr	24 hr	48 hr	72 hr	96 hr
Spermatogonia	221	146	94	74	62
Primary Spermatocytes	127	89	52	43	31
Secondary Spermatocytes + Round Spermatids	112	85	102	86	62
Elongating Cysts	784	834	722	736	705
Coiling Cysts	0	92	163	169	153
Total Cyst Number	1244	1246	1133	1108	1013

Table 2 continued: Quantification of viable different stage cysts in cultures treated with GSH at a concentration of 0.6 mg/ml, for cultures 3 and 4.

BSO Cyst Count Averages

BSO Average	0 hr	24 hr	48 hr	72 hr	96 hr
Spermatogonia	132	107	39	15	10
Primary Spermatocytes	113	27	3	0	0
Secondary Spermatocytes + Round Spermatids	102	109	84	75	68
Elongating Cysts	599	508	420	337	298
Coiling Cysts	0.0	84	87	63	59

Table 3: Average of the quantification tables for the three BSO-treated cyst cultures.
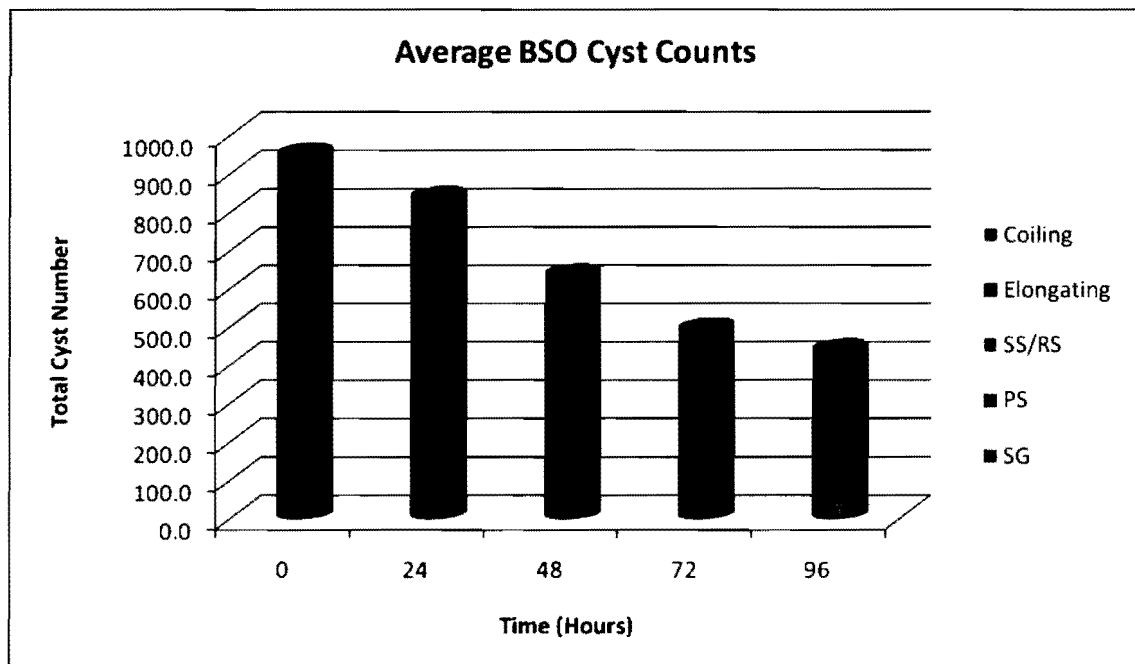
Figure 4: Graph of averages of the quantification tables for the three BSO-treated cyst cultures. Different cyst stages are indicated in color from the earliest, bottom of column, to the latest, top of column.

Control Cyst Count Averages

Control Average					
	0 hr	**24 hr**	**48 hr**	**72 hr**	**96 hr**
Spermatogonia	155	116	88	75	62
Primary Spermatocytes	103	77	53	42	24
Secondary Spermatocytes + Round Spermatids	95	76	76	61	49
Elongating Cysts	678	696	664	634	595
Coiling Cysts	0	63	110	111	124

Table 4: Averages of the quantification tables for the four control cyst cultures.
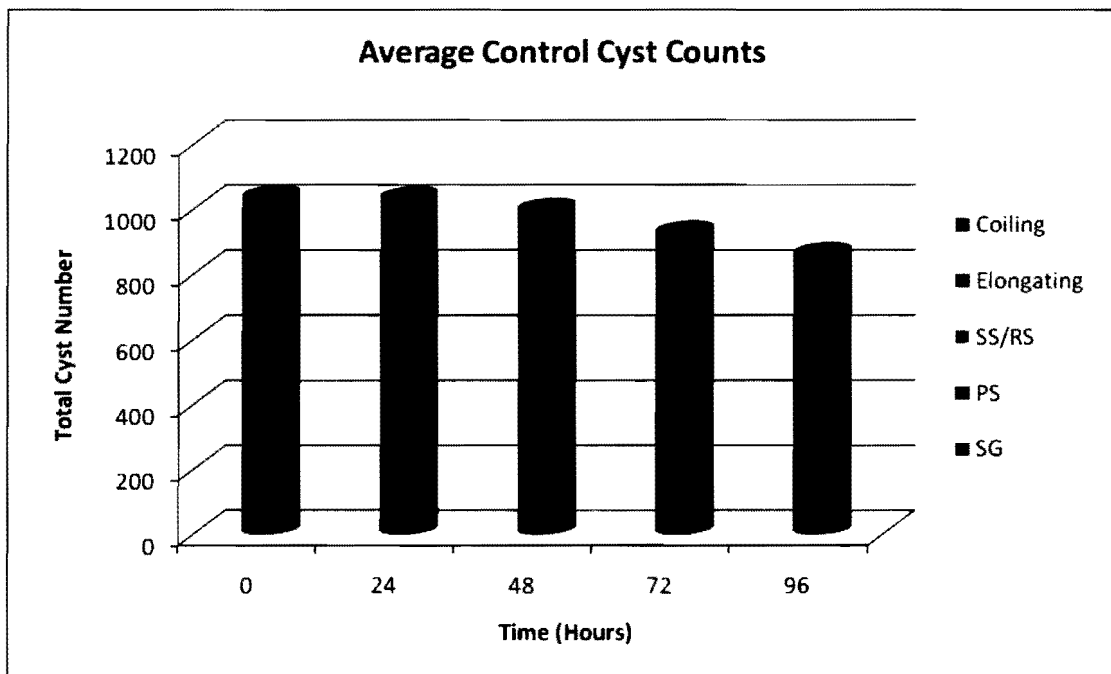
Figure 5: Graph of averages of the quantification tables for the four control cyst cultures. Different cyst stages are indicated in color from the earliest, bottom of column, to the latest, top of column.

BSO Cyst Percentages

Coiling
Elongating
SS/RS
PS
SG

Control Cyst Percentages

Coiling
Elongating
SS/RS
PS
SG
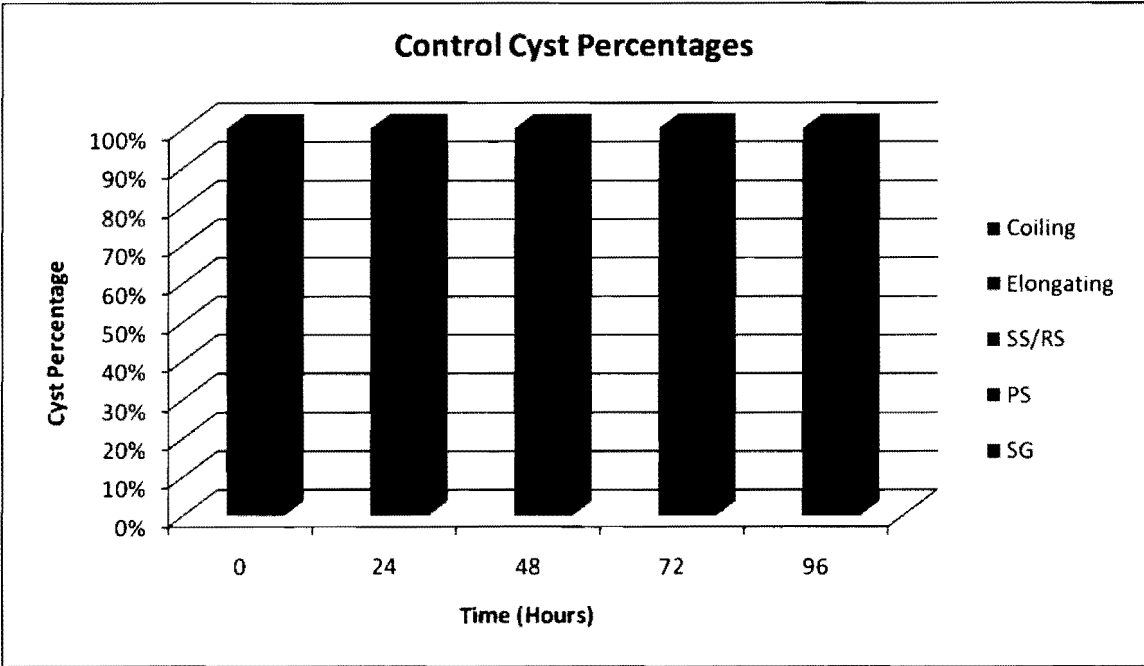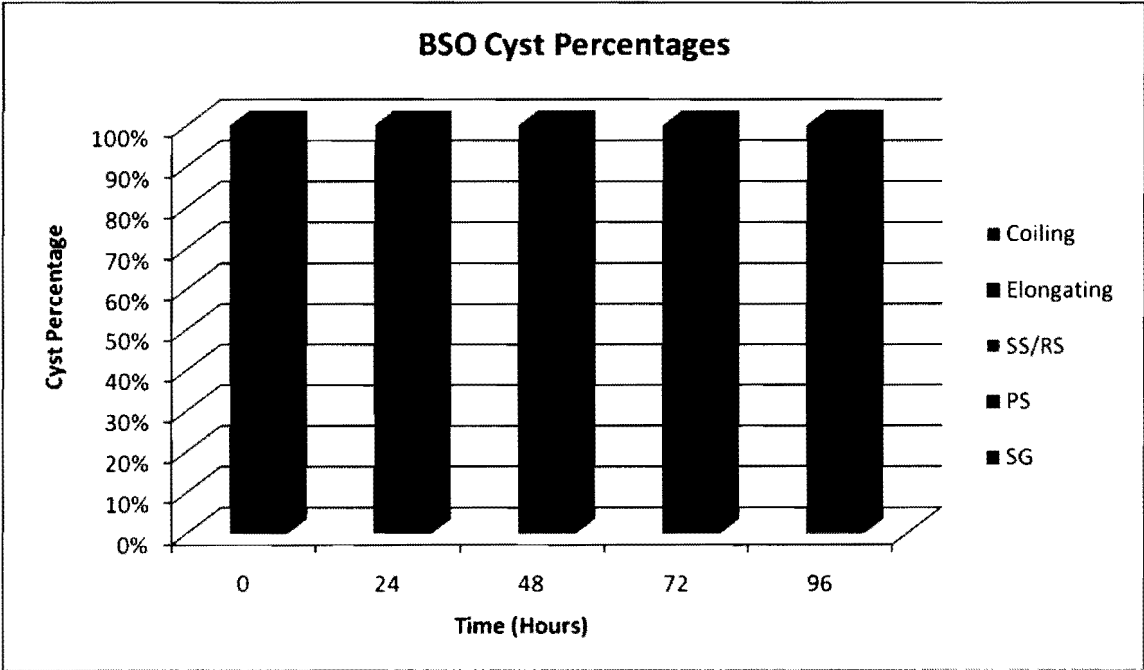
Figure 6: Percentages of surviving cysts with BSO above and control below. Different cyst stages indicated in color from earliest, bottom of column, to latest, top of column.
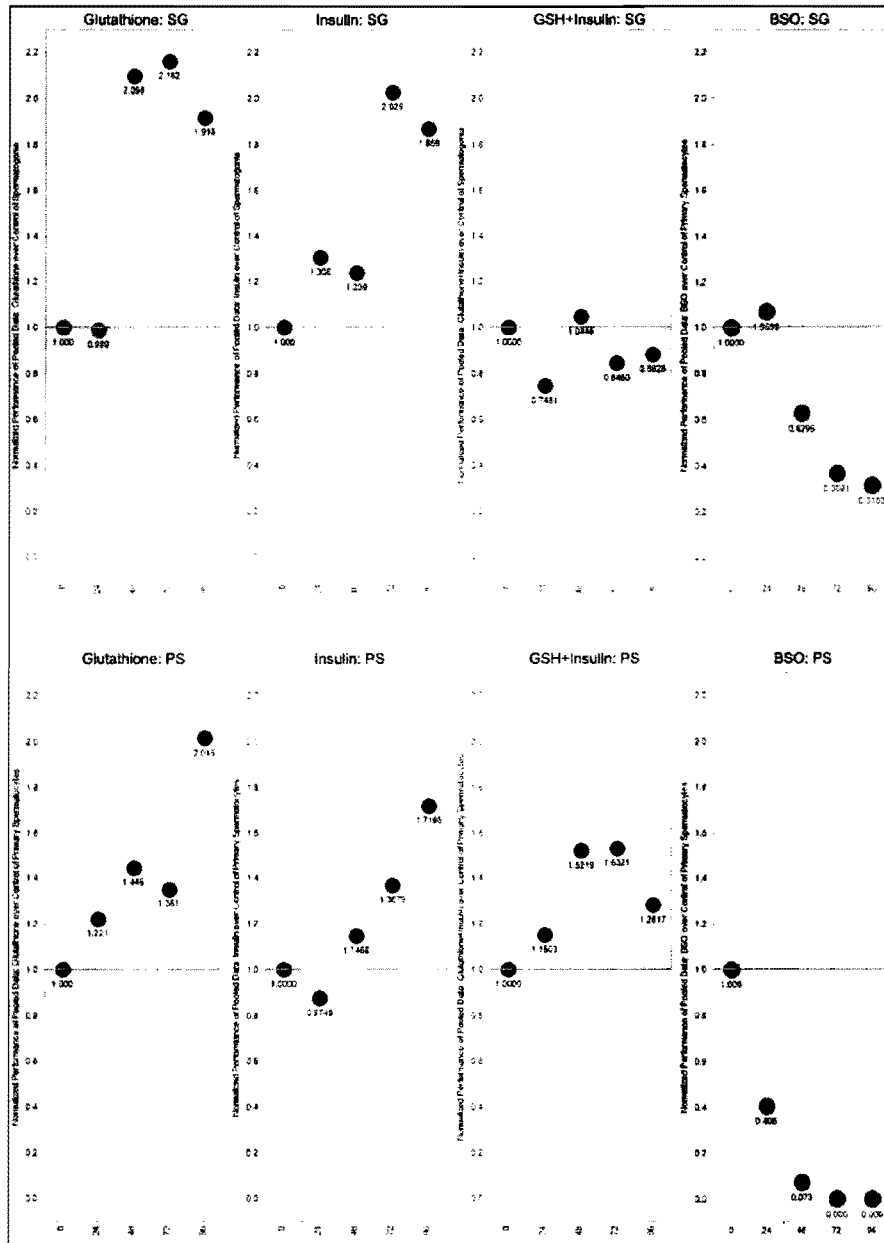
Figure 7: Performance factors for SG cysts (upper panel) and PS (lower panels) over 96 hours in culture. Performance was calculated by BSO cyst %/Control cyst %. GSH, insulin, and GSH+insulin data. (GSH, insulin, and GSH+insulin are as adapted from Ricketts *et. al.* 2011). Factors were normalized to 1 for Day 0.

26

II. Cultures of *Drosophila pseudoobscura* Cysts

We sought to determine the effects of BSO-induced oxidative stress on *in vitro* cultures of spermatogenic fly cysts. Cultures were set up using spermatogenic cysts isolated from *Drosophila pseudoobscura* pupae. BSO was used to assess the antioxidant effect of intracellular GSH on cyst development from 0 – 96 hours in culture. The effect of oxidative stress was analyzed by comparing the survival of cysts at different stages and by the presence of morphological cyst abnormalities between control cultures and the BSO experimental cultures. As shown in Figure 3, the different stages of fly spermatogenic cysts - SG, PS, secondary spermatocytes, round spermatids, elongating spermatids, and coiling sperm - were identified by the number of cells in each cyst type, size, and distinguishing morphological characteristics of each cyst stage.

Previous work from our lab found two cyst types that appear to be particularly susceptible to oxidative stress: SG and PS. Therefore the statistical analyses were concentrated on these cyst types. As shown in Tables 3 and 4, all 0 hour cultures had similar spermatogenic stage percentages with averages of 14-15% for SG, 10-12% for PS, 9-10% for secondary spermatocytes/round spermatids, and 63-65% for elongating cysts. There was no statistical difference in the starting percentages; the p-value was less than 0.05 of SG and PS cysts between the BSO and control cultures at the initiation of culture (Figure 8). Also on Day 0, no cysts at the coiling or individualizing stages were seen. The total number of cysts counted increased at 24 hours due to the dissociation of groups of elongating cysts that were previously uncounted at hour 0 (Tables 1 and 2).

The cysts in control and BSO cultures developed normally in the first 24 hours.

By 24 hours, the cysts were progressing through the stages of spermatogenesis and there were also cysts that had entered the individualization and coiling stages. Most of the cyst degradation, observed as grape-like bunches of cells, was seen as burst 32 SG or 32 PS cysts (Figure 9). There was no statistically significant difference between the loss of the earliest spermatogenic cysts; the 8-32 SG, until 48 hours (Figure 8), and the percentages of SG in both cultures remained about the same at 14% and 15%, respectively (Table 6). For the PS cysts, there is a statistically significant decrease between the BSO and control cultures, with a p-value < 0.05, after 24 hours. This statistical decrease was accompanied by a large increase in the appearance of the grape-like bunches as described earlier.

As shown in Tables 3 and 4, the percentages of SG and PS cysts in BSO and control cultures at 48 hours were similar to those at 24 hours. The control cultures showed cyst progression into the later stages of spermatogenesis while having slightly more degradation of PS in the form of grape-like bunches as well as signs of degradation of some elongating cysts and coiled sperm; however, the BSO culture was vastly different from the control culture. The BSO culture contained an extremely high amount of degradation of PS cysts with this cyst stage disappearing completely in some cultures due to cyst cell degradation.

In the 48-hour cultures, the PS continued to degenerate at an increased level with percentages dropping to < 1%. The difference in the degradation of PS, as observed in the 24-hour count, was significant between the BSO and control cultures with a p-value of < 0.05. Also at 48 hours, an increase in the degeneration of SG cysts was observed, dropping to 6% of the total cyst number. The percentage of SG cysts in the BSO cultures

was significantly less than that of the control with a p-value of < 0.05, and cyst

percentages of 3% and 0% respectively. The statistical significance of the SG and PS

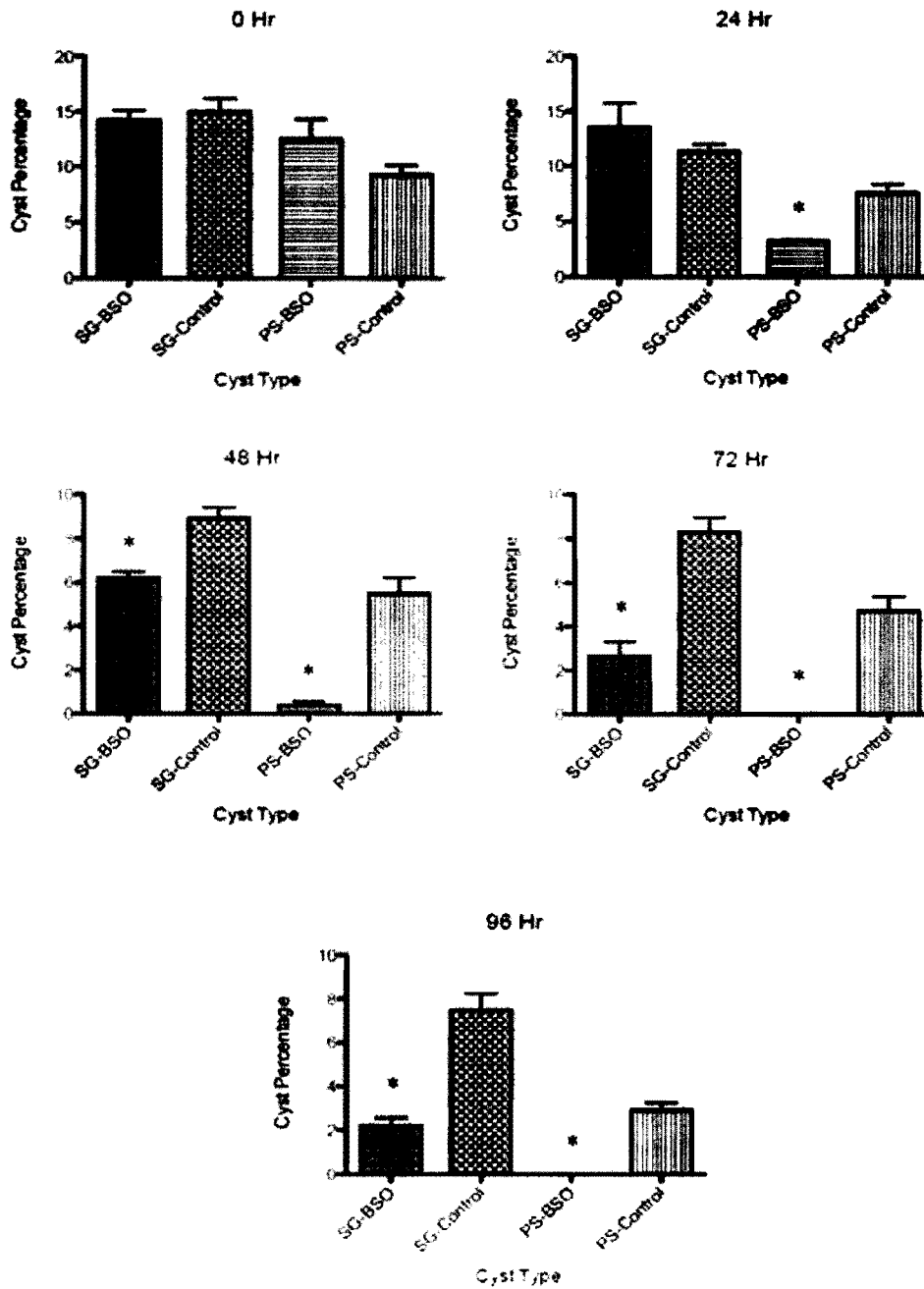cysts in BSO cultures trended from 48 hours through 96 hours.

Figure 8: Two-tailed t-test graphs comparing cyst types, SG and PS, from the BSO and Control during 0-96 hours of culture. Statistical significance, p-value < 0.05, is indicated by an asterisk.

30

The 72-hour observation and cell count showed an increased degradation in both the BSO and control. The increase was seen in the BSO culture through the complete disappearance of viable PS cysts and a great increase in the degradation of SG cysts (Figures 4, 6, and 8). The control cyst cultures also showed a decrease in the viability of SG and PS cysts, though to a much lesser degree. The BSO culture stayed statistically different from the control culture in terms of SG percentage and PS percentages with p-values < 0.05, respectively. The 3.6% decrease in the percentage of SG cysts in the BSO cultures was much greater than the 0.6% decrease seen in control cultures, leading to the increase in statistical significance and p-values <0.05. At 72 hours, differences between the cyst development and degradation appeared between the BSO and control cultures.

The BSO cultures had a large number of round cysts that seemed bloated and transparent, with the cysts intact and the cells within degraded (Figure 9). This abnormality was rarely seen in control cultures, even at 96 hours. Also in the BSO cultures, abnormalities appeared in some elongating cysts where the spermatids were irregularly elongating, resulting in odd bulbous cysts with portions protruding out (Figure 9). At 96 hours, both cultures showed elevated degradation, with BSO cultures showing vast degeneration (Figures 4 and 5). They also possessed elevated degradation in comparison to 72 hours; however, the increase was minimal. The BSO cultures were still significantly lower than the control cultures with p-values < 0.05 for SG and PS, respectively. At 96 hours, the BSO cultures were still significantly lower than the control cultures with p-values < 0.05, for SG and PS cysts.
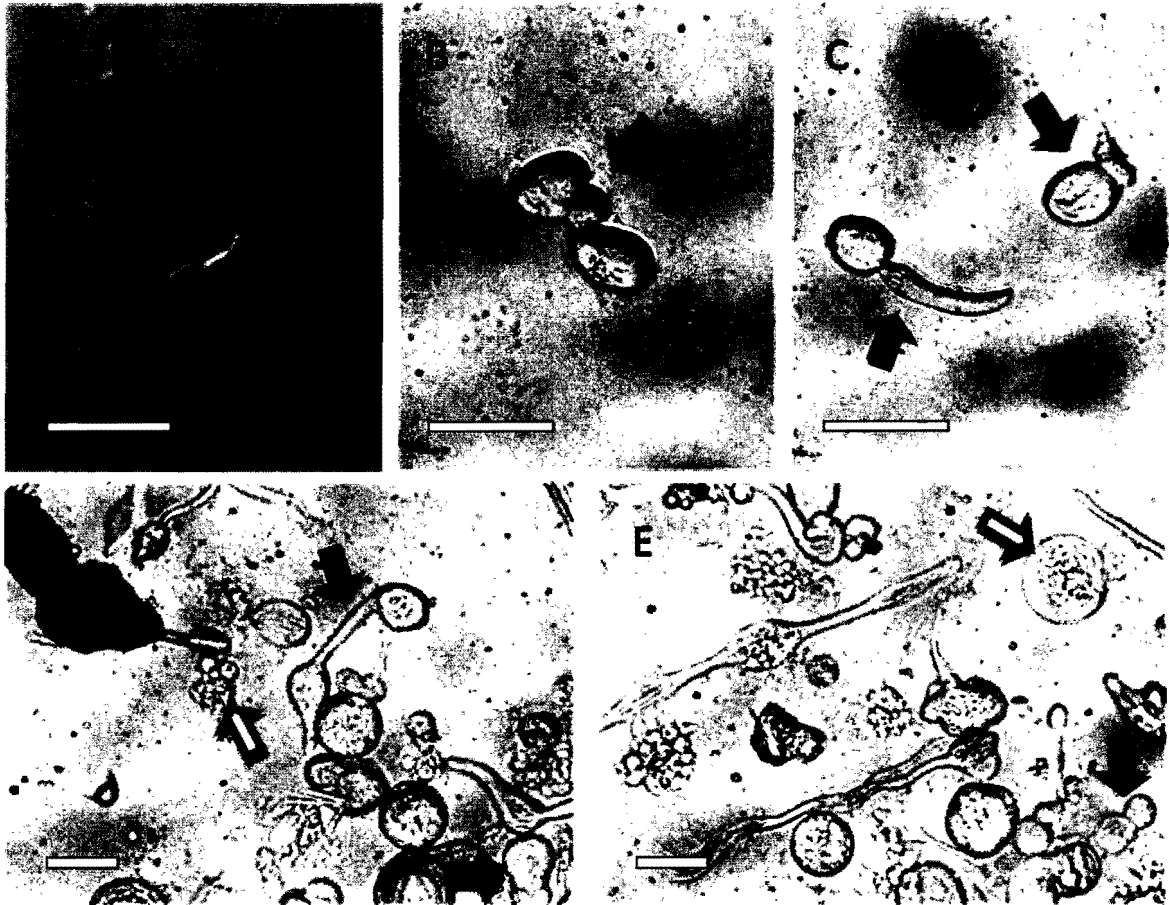
Figure 9: Cyst abnormalities and degeneration in BSO cultures at 72 hours. In panels A-E, several forms of abnormalities and degeneration are depicted. Blue arrows indicate abnormal elongation, magenta arrows indicate uneven or abnormal mitotic/meiotic divisions. The yellow arrows mark degeneration with cyst cell degeneration being indicated in panel D and developing spermatogenic cell degeneration in E. Scale bars = 100 μm.
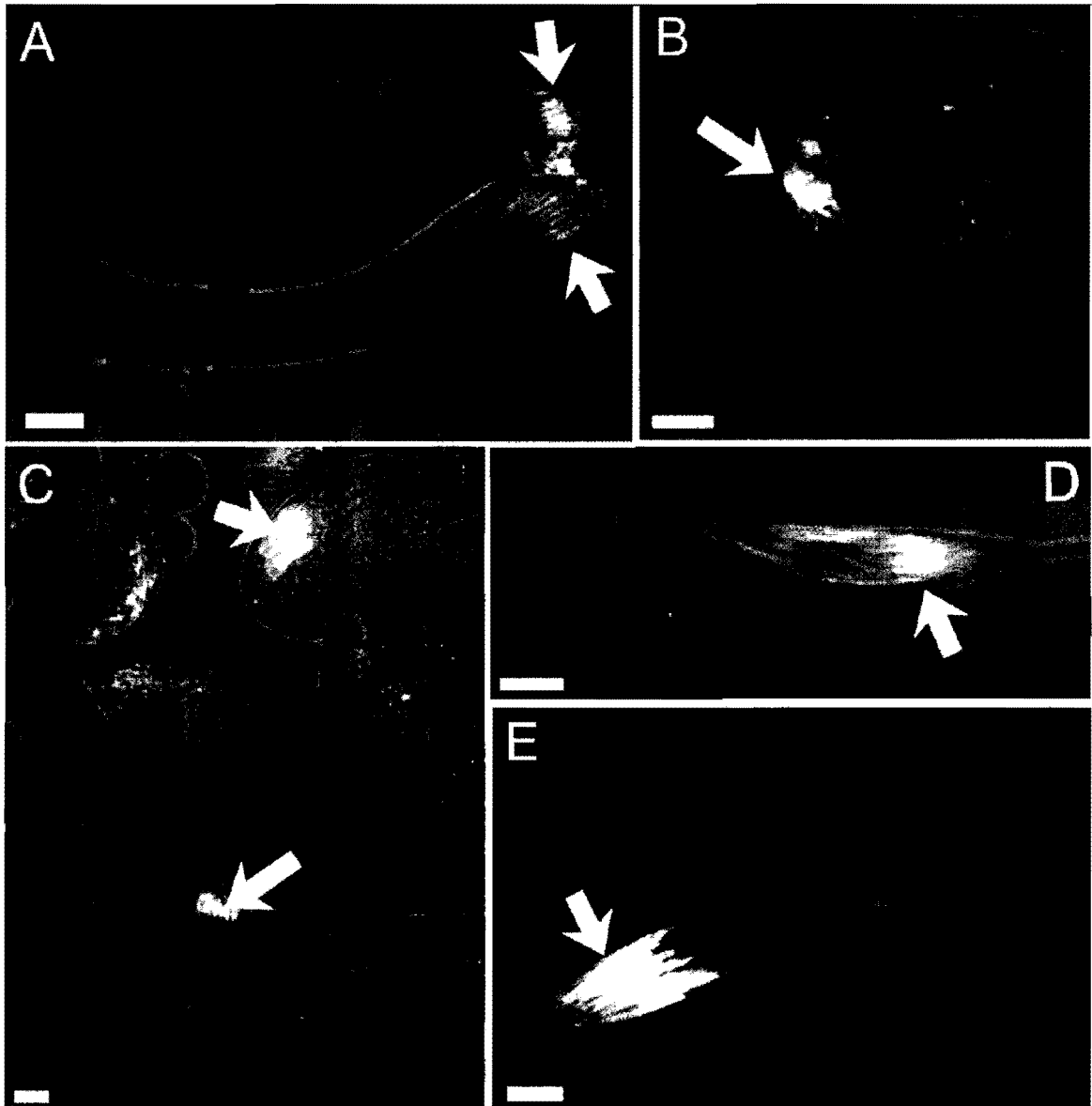
Figure 10: Brightfield images of cultured cysts with fluorescent signal from nuclei (arrows) overlaid. (A) Examples of normal elongating cysts after 24 hours in GSH-treated culture. (B–E) Abnormal cysts present after 72 hours in BSO-treated cultures. Several different types of abnormally elongating cysts were observed. In some cases, the nuclei appeared to begin elongation, but became disorganized (large arrows, B and C), while the elongation of the tail portion of the cysts was retarded. Some cysts at the pre-elongation, round spermatid stage also exhibited disorganized nuclei (small arrow, C). D and E show cysts with normally elongating nuclei (arrows), but abnormally developed tail regions of the cysts. (As adapted from Ricketts *et. al.* 2011).

33

III. Performance Factor

A performance factor was calculated to determine the extent of cyst degradation in BSO cultures. The performance factor data is shown in Figure 7. Cyst performance for BSO cultures was compared with data for insulin and GSH, collected previously (Ricketts *et. al.* 2011). Performance factor analysis compared the ratio of experimental SG and PS cysts with the control to determine survivability of the cyst stages in the BSO cultures. A performance factor >1 indicates that the experimental performed better than the control whereas a performance factor <1 indicates the experimental performed worse than the control. The analysis indicates that SG cysts in BSO cultures consistently performed below the control after the Day 0 count. In the top graph, the SG performance data shows a slight increase at 24 hours and a decrease below the performance of the control from 48-96 hours. The PS performance data in the bottom graph of Figure 7 shows PS cultures performed worse than the control from 0-96 hours.

IV. Ultrastructural Analysis of *D. pseudoobscura* Testes

As mentioned previously, the testes of *D. pseudoobscura* are morphologically very different from the model species *D. melanogaster*. The structure of *D. melanogaster* testes has been studied in detail (Tokuyasu 1972). However, the morphology and ultrastructure of *D. pseudoobscura* has, to this point, gone uninvestigated. Transmission electron microscopy was utilized to investigate the details of *D. pseudoobscura* testis ultrastructure. In particular, we were interested in the association of the elongating cysts with the basal epithelium, as previous work in our lab (Njogu *et. al.* 2010) indicated that the basal epithelium appears to play a role in cyst coiling and sperm motility.

34

Figure 11 shows the outer membrane of the testes, which is approximately 2.5 to 3 microns thick. This cell layer has a large number of pigment granules, ranging in size up to a ¼ micron in size (black arrows, Figure 11). The granules also appeared to be evenly distributed within the membrane cells. Also, within the outer membrane cells, there were ducts or tubes representing the trachea (yellow arrow, Figure 11). The tubes are invaginated around their edges and appeared to be surrounded by slightly more electron-dense areas of the membrane cells. The outer tissue layer was tightly associated with what appeared to be a layer of smooth muscle. Within the layer of smooth muscle, there are portions that are electron-dense within the cell layer as indicated in Figure 11C.

Further analyses of the testes focused on around cyst development, nuclear condensation, and cyst embedment in the basal epithelium. Figure 12 shows several cysts at different stages of development. The individual sperm in the cysts appeared as three adjacent circles due to the formation of several structures. The condensing nucleus, forming mitochondrial sheath, and the 9+2 microtubule arrangement of the tail, make up the cross-section seen in Figure 12's A and B. The mitochondrial sheath surrounding the mid-piece of the developing spermatid is comprised of two derivatives: a major mitochondrial unit and a minor mitochondrial unit as seen in Figures 12 and 13. The major mitochondrial units are the round areas of highest electron density, while the minor mitochondrial units are the adjacent, round, and slightly-less electron-dense areas (Pasini 1996). In this same figures (12 and 13), these two are arranged above the forming tail, all together forming cross-section formation. The cysts are known to have entered the elongation state due to the above characteristics of the sperm cells.
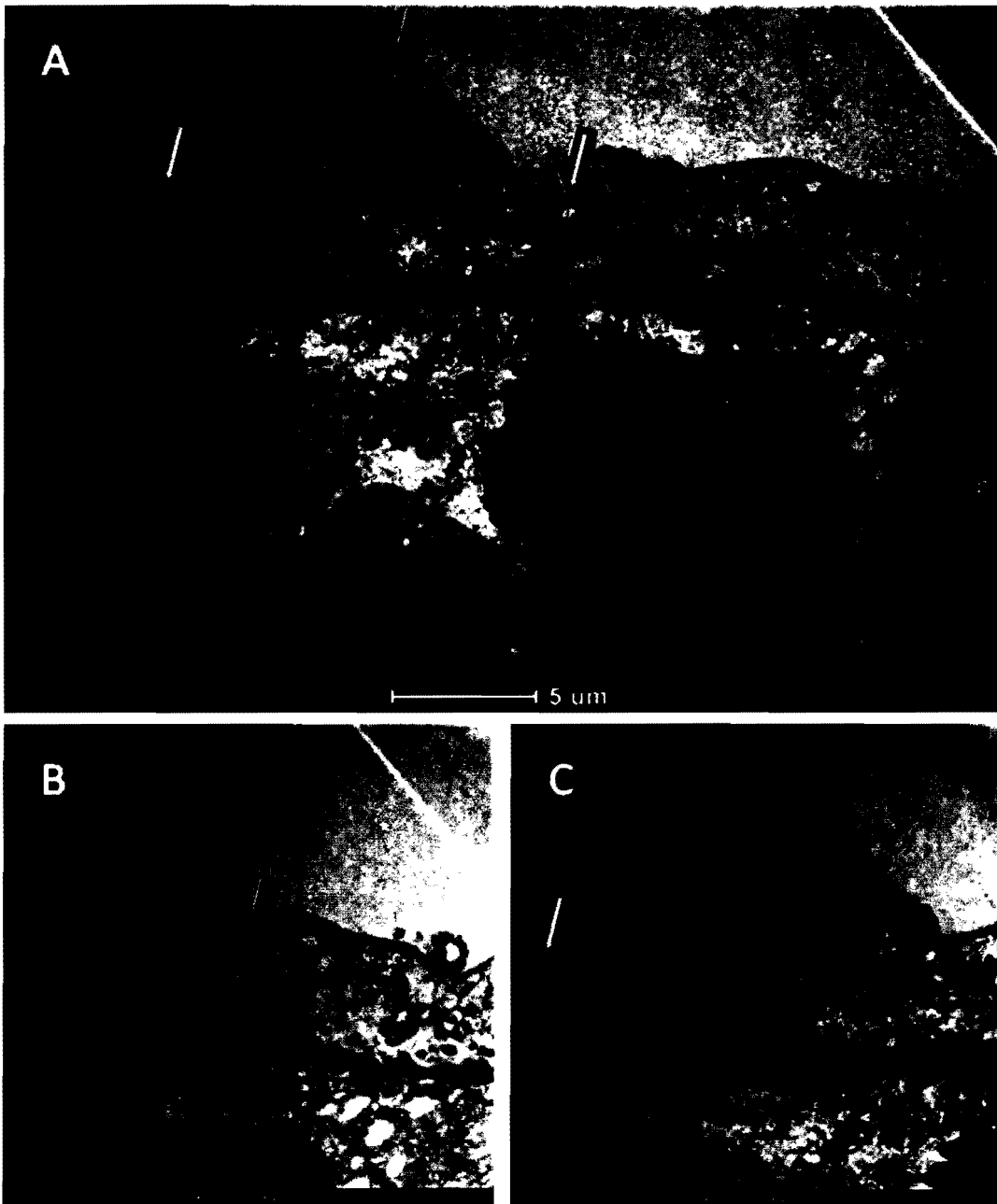
Figure 11: TEM of *D. pseudoobscura* pupal testes showing the outer epithelium. Yellow arrows indicate trachea within outer epithelium, red arrows indicate muscle layer, black arrows indicate pigment granules, and the blue arrow indicates Z-disc. A is an image of outer epithelial layer in close proximity to cysts. B and C are close-up sections of A.
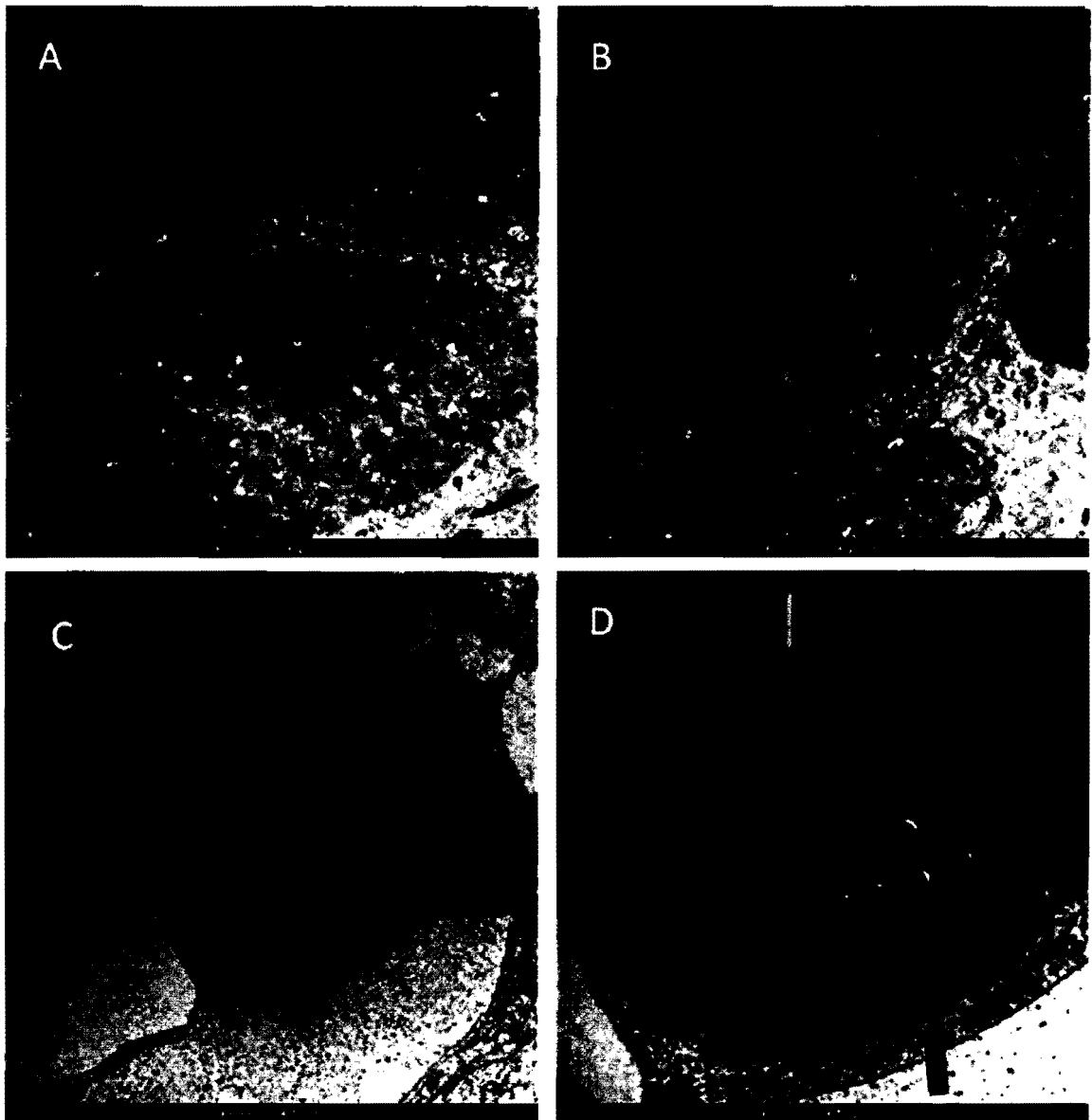
Figure 12: TEM micrographs of *D. pseudoobscura* pupal testes showing cyst shape and condensation. Condensing cysts are seen in panels A and B with later-stage cysts being more electron-dense. A fully condensed cyst is shown in panel C, and a close-up is shown in panel D. The 9+2 microtubule organization (green), the major mitochondrial derivative (yellow), and minor mitochondrial derivative (red) are shown in Panel D.

Once the elongation stage commenced, the cysts in *D. pseudoobscura* were loosely organized in an ellipsoid shape (Figure 12). As the cells within the cyst progressed through elongation, condensation of the nucleus and mitochondrial sheath is mirrored by overall cyst condensation changing the shape of the cyst from ellipsoid to a much more rounded shape. In the completely condensed cyst, the nucleus is extremely electron-dense and is about half as large in diameter as the tail (Figure 12). The mitochondrial derivatives (small and large), adjacent to the nucleus, was about a quarter of the size in diameter, and was more electron-dense in comparison to the nucleus. The extreme condensation of the cyst is demonstrated by the close relationship between the cyst cell between outer sperm cells as shown in Figure 12D.

The interaction between cyst and the basal epithelium has been reported in *D. melanogaster* (Tokuyasu 1974). This interaction has been visualized by TEM and is important in the coiling that occurs at the end of spermatogenesis. In *D. pseudoobscura*, there is evidence of a similar embedding event, which occurs at the basal end of the testes. In Figure 13A, a cyst is shown mostly surrounded by an electron-dense structure, which may represent two double membranes: one of the cyst cells and one of the basal epithelial cells. The same electron dense structure also surrounds the condensed cyst seen to the upper left in Figure 13A. A large space opposite the electron dense structure was often observed (Figures 12C and 13A). In Figure 13C, there appear to be two membranes, which are both membranes of the cyst cell, separating the actual sperm from the electron-dense membrane. Within the cyst, small round electron-dense structures were seen throughout the spaces between the sperm, and are assumed to be microtubules,

38

as seen in Figure 13C.

As shown in Figure 14, there appears to be thin, linear, electron dense structures, assumed to be plasma membranes surrounding the majority of the developing sperm. There is also the presence of excess cytoplasm and the lack of extreme condensation when compared to the cysts shown in Figure 12 (panels C and D), indicating the cyst shown in Figure 14 is earlier in the elongation process. Figure 14C and D show that the electron dense structure does surround individual sperm and in between sperm within the cyst seen as gaps indicating there are two membranes side by side (Figure 14D).
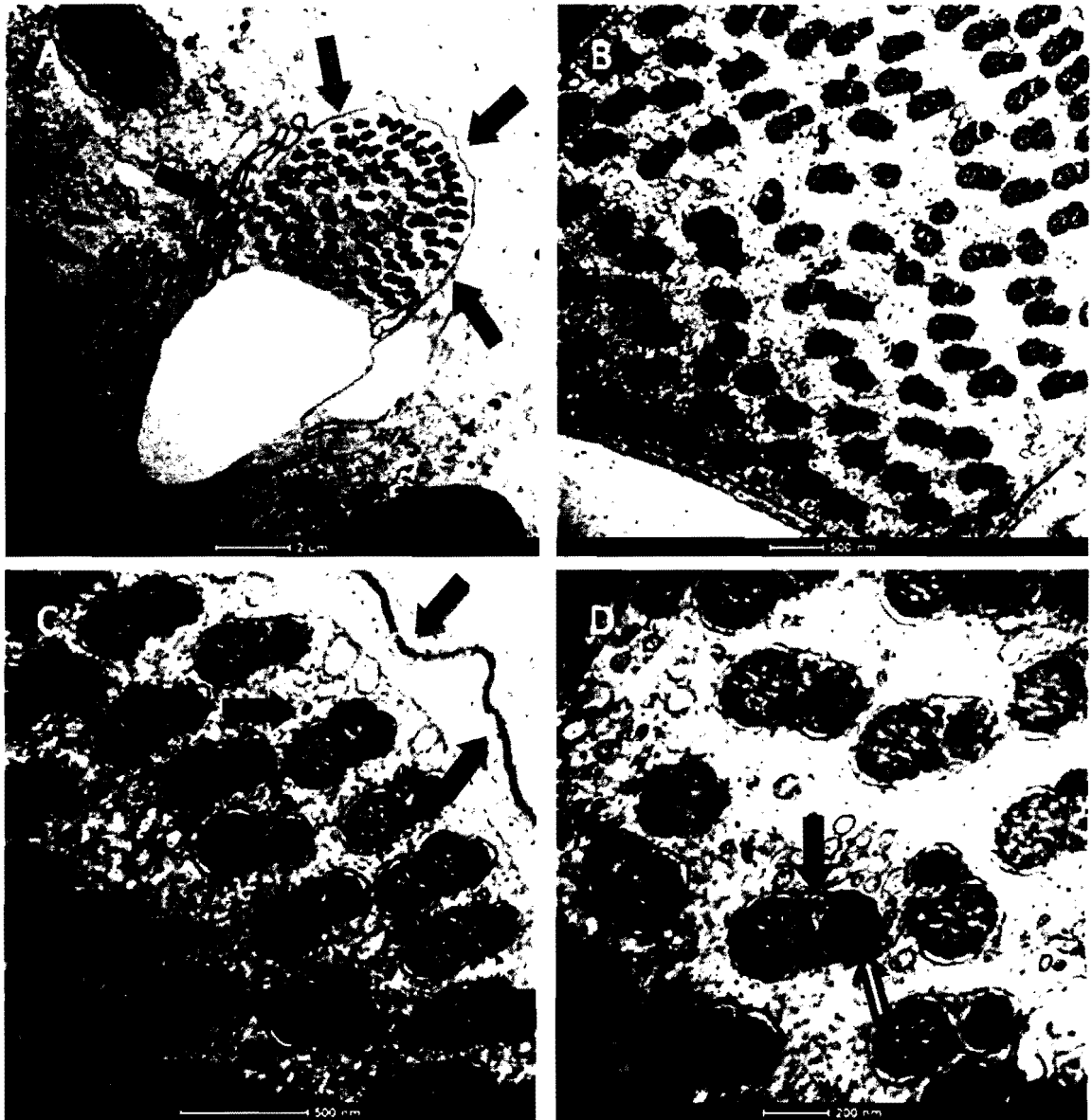
Figure 13: TEM micrographs of *D. pseudoobscura* pupal testes showing cyst embedding into basal epithelium. Panel A shows the cyst embedding into the basal epithelium with an electron-dense structure (green arrows) defining the relationship between the membrane of the head cyst cell and the epithelial cell. Panel C shows a close-up of this membrane complex indicated by green arrows. Microtubules are indicated by the blue arrows. The major mitochondrial derivative (yellow) and minor mitochondrial derivative (red) are indicated in D.
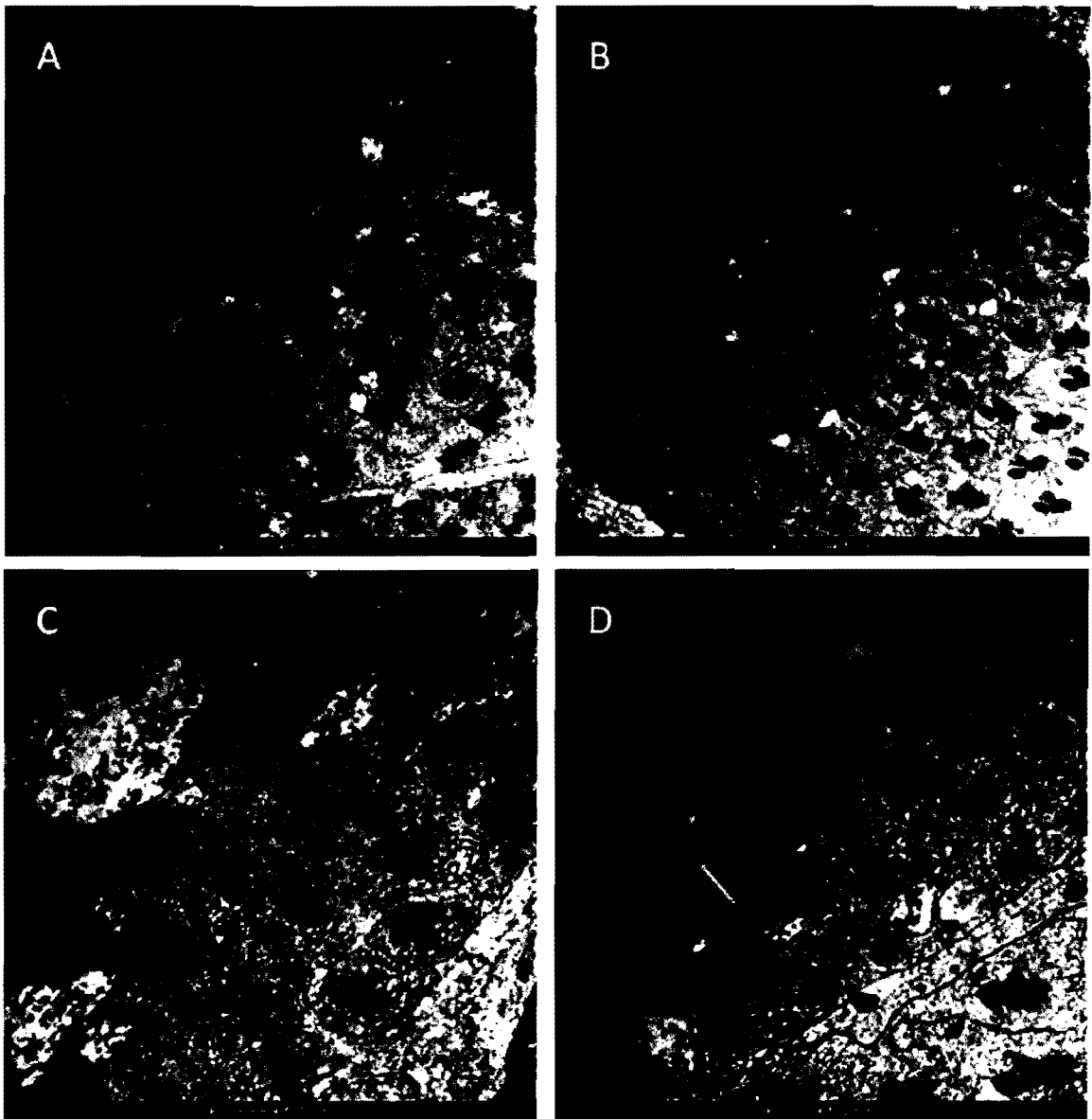
Figure 14: TEM micrographs of *D. pseudoobscura* pupal testes showing plasma
membranes around individualizing sperm. In Panels A and B, there appear to be plasma
membranes surrounding individual sperm within the cysts. Panels C and D are close-ups
of the cells shown in A and B. Individual distinct plasma membranes, indicated by two
lines between each sperm (green and yellow arrows), are seen surrounding the sperm.

Discussion

I. Effect of Oxidative Stress on Spermatogonia and Primary Spermatocyte Cysts

Our results indicate that the addition of BSO to our cyst culture system has a significant effect on the degeneration of early spermatogenic cysts, specifically SG and PS. Statistical analysis and performance factor analysis both showed a significant decrease in these cyst types over the course of 96 hours in culture. The PS cysts appeared particularly susceptible to degradation with those types completely disappearing from culture by 48 hours. These results indicate that BSO successfully shuts off the intracellular production of GSH and therefore effectively removed the cells main antioxidant system causing increased degeneration and greatly increased abnormal cyst morphology and development when compared to controls.

Reaction oxygen species are the cytotoxic by-products of the many cellular processes that metabolize oxygen (Kanzok 2001). There are, in essence, two systems for GSH production in the cell: its *in vivo* synthesis and the reduction of GSSG, which are two GSH molecules bound together after reducing a ROS.

Glutathione, or γ-L-glutamylcysteinylglycine, is produced intracellularly through several consecutive steps of combining its constituent amino acids in their correct order and orientation. First, glutamine is processed and bound to cystine, by γ-glutamylcysteine synthetase (GCS), for the formation of γ-glutamylcysteine. Then, glycine is bound to γ-glutamylcysteine by GSH synthetase to form γ-L-glutamylcysteinylglycine (Anderson 1998). The enzymatic reaction mediated GCS is the rate limiting step in intracellular production of GSH. In mammals, GCS has two subunits: a 73 kDa heavy subunit and a

30 kDa light subunit (Saunders 2000). Intracellular production of GSH is regulated by the light subunit and feedback inhibition of GSH (Anderson 1998). The second source of GSH production is its reduction from GSSG by glutathione reductase and the reducing power of NADPH. In *Drosophila,* there is no true glutathione reductase system responsible for reducing GSSG to GSH. Instead, the thioreduction system replaces the glutathione reductase system in maintaining proper redox levels of GSH in the cell (Missirlis 2001).

GSH can be effectively inhibited by introducing the chemical, BSO, to cells *in vitro* (Anderson 1998). BSO inhibits the rate limiting enzyme, GCS, in the GSH synthesis pathway. The introduction of this chemical was seen to reduce cellular GSH levels to 10-20% of the control levels (Anderson 1998).

The insights into the importance of GSH in spermatogenesis are reflected by previous GSH studies (Ricketts *et. al.* 2011) and in the data gathered in the current work. In the BSO experiments, there was a definite and significant decrease in the viability of PS and SG, respectively. The SG and PS cysts are the two earliest cyst stages in *Drosophila* spermatogenesis. At these stages of spermatogenesis, the cysts have not entered the second meiotic phase which is characterized by much higher transcriptional activity (Vibranovski 2010). It is possible that at these stages, the cells have not yet synthesized high levels of GSH. This combination of factors may lead to more susceptibility to oxidative stress than the other cyst types. This idea is reflected by the significant decrease of the PS cysts in BSO cultures starting at 24 hours and their disappearance from culture at 72 hours, and the SG cysts significant decrease in the BSO

43

cultures starting at 48 hours.

The delay in the observed effect of the BSO induced oxidative stress may be because there has already been some synthesis of GSH in the cells, although the amount may be very low. The intracellularly-produced GSH would be active as an antioxidant and could reduce ROS and be recovered by glutathione reductase and NADPH. However, the suggested low levels of GSH in the SG and PS cyst types would be unable to handle the antioxidant workload of the SG cells undergoing many cell divisions in a short time. Given the speculation above, it would not be unreasonable to suggest that the cyst stage to be most effected by oxidative stress would be the SG cysts because they have had the least time to produce GSH and are not as transcriptionally-active as other cyst types. However, our data suggest that PS cysts are the cyst type most affected by oxidative stress. In fact, by 48 hours the PS are essentially eliminated from the BSO cultures with percentages of $< 1\%$, and the SG being $> 6\%$. There are many possible explanations for this phenomenon.

First, physical stress during the PS stage might make these cysts more susceptible to oxidative stress. Second, the PS cysts have higher metabolic activity than SG cysts, and thus would produce higher levels of ROS. During the PS cyst stage, developing spermatocyte cells increase their size up to approximately 25 times (Fuller 1998), putting great mechanical stress on the cyst cells encompassing them. Also, PS's are highly metabolically-active producing mRNAs for later stages of spermiogenesis. The mechanical stress and high metabolism may be reasons why the PS to are more susceptible to the degradation caused by oxidative stress and free radicals than the SG

44

cysts. Other than the PS and SG cysts, there was no significant difference between other cyst types when comparing the control to the BSO cultures.

Given the importance of GSH in the cell as the most abundant non-protein thiol with many critical functions (Markovic 2007), studying GSH in conjunction with complex cellular processes such as spermatogenesis is warranted. Cotgreave *et. al.* (1998) investigated the connection between GSH, cell proliferation, and apoptosis. They observed that mitosis and apoptosis are linked to oxidants and oxidant mediated regulation. These authors noted that the overall mechanism and involvement of antioxidants in proliferation is undoubtedly complex. However, it is known that cell proliferation is induced at low levels of oxidants (Cotgreave *et. al* 1998), therefore it is reasonable to assume that the redox state of GSH has some effect on the cell's ability to enter into mitosis, although its role may differ depending on cell type. In the current work, the cyst types most affected by oxidative stress were those involved in mitotic and meiotic cell proliferation (SG and PS, respectively). Furthermore, GSH and spermatogenesis appear to be more intertwined because of the recruitment of GSH into the nucleus during cell division (Markovic 2007).

Although SG and PS are the only cyst types to have a significant decrease in BSO cultures, there were other signs of the oxidative stress on several other cyst types. These abnormalities in BSO cyst cultures came in three forms not seen in the control cultures. First, there was a high occurrence of the spermatogenic cells within the cysts degenerating while the cyst cells stayed viable. This is different from the control where the main degeneration was seen in the cyst cells and the formation of the grape-like

45

bunches. This suggests that the spermatogenic cells were more susceptible to oxidative stress than the cyst cells. Some inferences can be made from this observation. The degeneration seen in the controls is most likely due to physical stress rather than oxidative stress, which may explain why PS cysts seem to degrade more than the SG cysts in BSO cultures. It is possible that the cyst cells are more transcriptionally-active at the early spermatogenic stages and produce more GSH than the SG cells and are therefore more protected. Another abnormality observed in BSO cultures was the uneven or lopsided division of the SG cysts. Instead of all the cells within the cyst dividing equally and normally, the division seems uncoordinated with cysts forming prominent bulges of cells and lobules. This may be due to the suggested role of GSH in proliferation (Cotgreave 1998). The final, and possibly most intriguing, abnormality was the uneven and misplaced start of elongation as described below.

II. Effect of Oxidative Stress on Elongating Cysts

In normal spermatogenesis, elongation starts in all cells equally and leads to a coordinated elongation along the whole cyst as shown in Figure 10A. However in the abnormal cysts, this coordination was lost. Elongating portions of the cysts were seen to protrude out of a round or abnormal portion of the cyst. This seems to indicate the cyst cells were not elongating properly, and the cause may be with either the head or the tail cyst cell. Hoechst staining of the BSO treated cysts indicated that both the head and tail ends of the cysts are affected by oxidative stress. Our data suggest that there is a difference between the head and tail cyst antioxidant levels. The reason for this difference is unknown, but elongating cysts are more metabolically active than earlier cysts.

46

Assembling the axoneme, condensing and reorganizing the nucleus and cellular structures (Ricketts *et. al.* 2011) require a highly active cell creating more ROS. It may be the increased ROS in this stage that is the cause of the abnormalities. Our data suggests that the head cyst cell has a better antioxidant defense than the tail. This makes sense from an evolutionary standpoint in that the cyst responsible for the area of the developing sperm nucleus containing the genetic material would be more resilient against oxidative stress.

III. Ultrastructural Analysis of *D. pseudoobscura* Testes

D. melanogaster has been studied for many decades and the ultrastructure of its testes has been analyzed, with focus on various stages of spermatogenesis (Tokuyasu 1972, 1974, 1975). However, these same analyses have yet to be completed in *D. pseudoobscura*. Our work shows that in the *D. pseudoobscura* testis, there is a 4-5 micron thick outer epithelial layer that has an abundance of pigment granules and several trachea-like structures distributed throughout the epithelial layer which may function to circulate oxygen to the testes (Valdez 2001). Toward the interior of the testis, there is a distinct layer with an overall higher electron density than the outer epithelial layer. As Valdez (2001) found, there are also what appear to be z-discs in the layer below the pigment layer in *D. pseudoobscura*. This 0.25 - 0.75 µm thick layer appears to be a similar muscle layer. As in the Mexican fruit fly, which has testes of similar morphology, it is hypothesized that this muscle layer aids in the movement of developing cysts from the apical toward the basal end through peristalsis (Valdez 2001). This muscle layer appears in *D. melanogaster*; however, its role is possibly reduced due to the testes length

and its tube-like shape aiding in the movement of cysts toward the basal end.

In addition to investigating the epithelial layer of the testes, we focused on the morphology of the elongating cysts and their interaction with the basal epithelium. Tokuyasu *et. al.* (1974) studied this relationship and the coiling cysts of *D. melanogaster*. *D. melanogaster* cysts have a very specific shape as they elongate and develop. Cross-sectional views of elongating cysts appear in a loose hexagonal shape, and condense into a hexagon after individualization has occurred (Tokuyasu 1974). This is not mirrored in *D. pseudoobscura* where the cysts are in a circular or ellipsoid shape during early elongation and then condense into a circular shape after individualization has occurred. The reason for this difference is unknown and is not assumed to be due to morphological differences of the testes but may be species-specific.

Njogu *et al.* (2010) hypothesized that there is an interaction between the cyst cells and the basal epithelium that may affect the motility of mature sperm. The ultrastructural analysis of the *D. pseudoobscura* testes does give evidence that there is an interaction between the cysts and the basal epithelium as in *D. melanogaster* (Tokuyasu 1974). As shown in Figure 13, an elongating cyst is beginning to condense and a large, convoluted, electron-dense structure surrounds the cyst. This structure appears to be composed of two membranes between the inside of the cyst where the sperm are found and the electron-dense structure. The first membrane may be the inner membrane of the head cyst cell and the outer membrane is part of the electron-dense structure. This electron-dense structure is most likely representative of an interaction between the outer membrane of the head cyst membrane and the membrane of the basal epithelium. The tail cyst cell appears to be

located towards the large voids shown Figure 12C and Figure 13 A, B). This electron-dense structure between the head cyst cell and the basal epithelium was also reported by Tokuyasu *et. al.* (1974). Tokuyasu inferred that the cyst embeds into the basal epithelium which may act as a mechanism for coiling *in vivo*.

We also noted that microtubules appear to be interspersed in the spaces between the individual developing sperm (Figure 13D). The function of these microtubules may be to coordinate and organize the sperm when condensing and they may have an impact on the overall shape of the cyst during and after elongation.

In performing the cyst culture preparations for the experiments described in this work, we noted that individualizing cysts were never seen at the initiation of culture. This phenomenon was also noted by Njogu *et. al.* (2010) and Ricketts *et. al.* (2011). Due to this absence, it was assumed that cyst development simply had not reached the individualization stage in pupal testes. However, TEM imaging of pupal cysts now suggests that the cysts are in the individualization stage during pupal development. As shown in Figure 14, two different cysts appear to be undergoing the individualization event, as indicated by the presence of individual plasma membranes around each sperm. The presence of these cysts with plasma membranes indicates that individualization does occur in pupae. The reason why individualizing cysts are not seen at the initiation of culture may be that the individualizing cysts are already firmly embedded in the basal epithelium and are not released when we harvest the cysts from testes for culture. The simple rupturing of the testes would not release them from this epithelium and they

would not be found in cultures at initiation. After 24 hours in culture, individualization is frequently observed.

IV. Future Directions

In vitro cyst culturing with BSO has provided insight into the importance of GSH and its antioxidant ability on cells during spermatogenesis. A future focus will be mapping the localization of GSH synthesis during spermatogenesis using the reagent Cell Tracker Green. Cell Tracker binds directly to GSH in live cell cultures and has been shown to track GSH within the cell, including its recruitment to the nucleus during proliferation (Markovic *et. al.* 2007). Additionally, we will further investigate the relationship of the basal epithelium with the developing cysts, as well as the role of the putative microtubule structures found within developing cysts.

References

Allocati, N., Federici, L., Masulli, M., and Di Ilio C. 2009. Glutathione transferases in bacteria. *The FEBS Journal.* **276** (1):58-75.

Anderson, C.P., and Reynolds, C.P. 2002. Synergistic cytotoxicity of buthionine sulfoximine (BSO) and intensive melphalan (L-PAM) for neuroblastoma cell lines established at relapse after myeloablative therapy. *Bone Marrow Transplant* **30** (3): 135-140.

Anderson, M.E. 1998. Glutathione: an overview of biosynthesis and modulation. *Chemico-Biological Interactions* **111-112**: 1-14.

Arama, E., Agapite, J., and Steller, H. 2003. Caspase activity and a specific cytochrome c are required for sperm differentiation in *Drosophila*. *Developmental Cell* **4**: 687-697.

Atzori, L., Dypbukt, J.M., Hybbinette S.S., Moldéus, P., and Grafström, R.C. 1994. Modifications of cellular thiols during growth and squamous differentiation of cultured human bronchial epithelial cells. *Experimental Cell Research* **211**: 115-120.

Balhorn, R. 2007. The protamine family of sperm nuclear proteins. *Genome Biology* **8** (9). doi: 10.1186/gb-2007-8-9-227.

Blake, A.D. 2004. Dipyridamole is neuroprotective for cultured rat embryonic cortical neurons. *Biochemical and Biophysical Research Communications* **314**: 501-504.

Blokhina, O., Virolainen, E., and Fagerstedt, K.V. 2003. Antioxidants, oxidative damage and oxygen deprivation stress: a review. *Annals of Botany* **91**:179-194.

Cheng, C.Y., and Mruk, D.D. 2011. Regulation of spermiogenesis, spermiation and blood-testis barrier dynamics: novel insights from studies on Eps8 and Arp3. *Biochemical Journal* **435**: 553-562.

Cotgreave, I.A., and Gerdes, R.G. 1998. Recent trends in glutathione biochemistry – glutathione-protein interactions: a molecular link between oxidative stress and cell proliferation?. *Biochemical and Biophysical Research Communications* **242**: 1-9.

Cross D.P., and Sang, J.H. 1978. Cell culture of individual *Drosophila* embryos. I. development of wild-type cultures. *Journal of Embryology and Experimental Morphology* **45**: 161-172.

Cross, D.P., and Shellenbarger, D.L. 1979. The dynamics of *Drosophila melanogaster* spermatogenesis in *in vitro* cultures. *Journal of Embryology and Experimental Morphology* **53**: 345-351.

DeGraff, W.G., Russo, A., and Mitchell, J.B. 1985. Glutathione depletion greatly reduces neocarzinostatin cytotoxicity in Chinese hamster V79 cells. *The Journal of Biochemical Chemistry* **260** (14): 8312-8315.

Desai, B.S., Shirolikar, S., and Ray, K. 2009. F-actin-based extensions of the head cyst cell adhere to the maturing spermatids to maintain them in a tight bundle and prevent their premature release in *Drosophila* testis. *BMC Biology* 7:19.

Electron Microscopy Sciences. 2011. *EMbed 812 kit, Technical data sheets.* http://www.emsdiasum.com/microscopy/technical/datasheet/14120.aspx

Fabian, L., Wei, H., Rollins, J., Noguchi, T., Blankenship, J.T., Bellamkonda, K., Polevoy, G., Gervais, L., Guichet, A., Fuller, M.T., and Brill, J.A. 2010. Phosphatidylinositol 4,5-bisphosphate directs spermatid cell polarity and exocyst localization in *Drosophila*. *Molecular Biology of the Cell* **21**: 1546-1555.

Fisher Scientific. 2011. http://www.fishersci.com/ecomm/servlet/cmstatic?storeId=10652&ddkey=http:home

Fraser, J.A., Saunders, R.D.C., and McLellan, L.I. 2002. *Drosophila melanogaster* glutamate-cysteine ligase activity is regulated by a modifier subunit with a mechanism of action similar to that of the mammalian form. *The Journal of Biological Chemistry* **277** (2): 1158-1165.

Fuller, M.T. 1998. Genetic control of cell proliferation and differentiation in *Drosophila* spermatogenesis. *Seminars in Cell and Developmental Biology* **9**: 433-444.

Hardy, R.W., Tokuyasu, D.L., Lindsley, D.L., and Garavito, M. 1979. The germinal proliferation center in the testis of *Drosophila melanogaster*. *Journal of Ultrastructure Research* **69**: 180-190.

Jackson, G.R., Werrbach-Perez, K., Pan, Z., Sampath, D., and Perez-Polo, J.R. 1994. Neurotrophin regulation of energy homeostasis in the central nervous system. *Developmental Neuroscience* **16**: 285-290.

Kanzok, S.M., Fechner, A., Bauer, H., Ulschmid, J.K., Müller, H., Botella-Munoz, J., Schneuwly, S., Schirmer, R.H., and Becker, K. 2001. Substitution of the thioredoxin system for glutathione reductase in *Drosophila melanogaster*. *Science* **291** (5504): 643-646.

Kawamoto, T., Kawai, K., Kodama, T., Yokokura, T., and Niki, Y. 2008. Autonomous differentiation of *Drosophila* spermatogonia *in vitro*. *Development, Growth & Differentiation* **50**, 623-632.

Kocháryová, M., and Kollárová, M. 2008. Oxidative stress and thioredoxin system. *General Physiology and Biophy*sics **27**: 71-84.

Kracklauer, M.P., Wiora, H.M., Deery, W.J., Chen, X., Bolival, B., Jr., Romanowicz, D., Simonette, R.A., Fuller, M.T., Fischer, J.A., and Beckingham, K.M. 2010. The *Drosophila* SUN protein Spag4 cooperates with the coiled-coil protein Yuri Gagarin to maintain association of the basal body and spermatid nucleus. *Journal of Cell Science* **123**: 2763-2772.

Krzywanski, D.M., Dickinson, D.A., Iles, K.E., Wigley, A.F., Franklin, C.C., Liu, R., Kavanagh, T.J., and Forman, H.J. 2004. Variable regulation of glutamate cysteine ligase subunit proteins affects glutathione biosynthesis in response to oxidative stress. *Archives of Biochemistry and Biophysics* **423**: 116-125.

Lee, S., Zhou, L., Kim, J., Kalbfleisch, S., and Schöck, F. 2008. Lasp anchors the *Drosophila* male stem cell niche and mediates spermatid individualization. *Mechanisms of Development* **125**: 768-776.

Liebmann, J.E., Hahn, S.M., Cook, J.A., Lipschultz, C., Mitchell, J.B., and Kaufman, D.C. 1993. Glutathione depletion by L-buthionine sulfoximine antagonizes taxol cytotoxicity. *Cancer Research* **53** (9): 2066-2070.

Lo, K.C., and Domes, T. 2011. Can we grow sperm? A translational perspective on the current animal and human spermatogenesis models. *Asian Journal of Andrology*: 1-6. doi: 10.1038/aja.2011.8.

Markovic, J., Borrás, C., Ortega, Á., Sastre, J., Viña, J., and Pallardó, F.V. 2007. Glutathione is recruited into the nucleus in early phases of cell proliferation. *The Journal of Biological Chemistry* **282** (28): 20416-20424.

Markow, T.A., and O'Grady, P.M. 2007. *Drosophila* biology in the genomic age. *Genetics* **177**: 1269-1276.

Meister, A. 1991. Glutathione deficiency produced by inhibition of its synthesis, and its reversal; applications in research and therapy. *The Journal of Pharmacology and Experimental Therapeutics* **51**: 155-194.

Missirlis, F., Phillips, J.P., and Jäckle, H. 2001. Cooperative action of antioxidant defense systems in *Drosophila*. *Current Biology* **11**: 1272-1277.

Moreira, J., Araújo, V.A., Báo, S.N., and Lino-Neto, J. 2010. Structural and ultrastructural characteristics of male reproductive tract and spermatozoa in two Cryptinae species (Hymenopera: Ichneumonidae). *Micron* **41**: 187-192.

Niki, Y., Yamaguchi, T., and Mahowald, A.P. 2006. Establishment of stable cell lines of *Drosophila* germ-line stem cells. *Proceedings of the National Academy of Sciences* **103** (44): 16325-16330.

Njogu, M., Ricketts, P., and Klaus, A.V. 2010. Spermatogenic cyst and organ culture in *Drosophila pseudoobscura*. *Cell and Tissue Research* **341** (3):453-464.

Phillips, B.T., Gassei, K., and Orwig, K.E. 2010. Spermatogonial stem cell regulation and spermatogenesis. *Philosophical Transactions of The Royal Society B: Biological Sciences* **365**: 1663-1678.

Rebrin, I., and Sohal, R.S. 2008. Pro-oxidant shift in glutathione redox state during aging. *Advanced Drug Delivery Reviews* **60** (13-14): 1545-1552.

Ricketts, P.A., Minimair, M., Yates, R.W., and Klaus, A.V. 2011. The effects of glutathione, insulin and oxidative stress on cultured spermatogenic cysts. *Spermatogenesis* **1** (2):159-171.

Russo, A., DeGraff, W., Friedman, N., and Mitchell, J.B. 1986. Selective modulation of glutathione levels in human normal *versus* tumor cells and subsequent differential response to chemotherapy drugs. *Cancer Research* **46**: 2845-2848.

Saunders, R.D.C., and McLellan, L.I. 2000. Molecular cloning of *Drosophila* γ-glutamylcysteine synthetase by functional complementation of a yeast mutant. *FEBS Letters* **467**: 337-340.

Sigma-Aldrich. 2010. *Glutathione in cell culture*. http://www.sigmaaldrich.com/life-science/cell-culture/learning-center/media-expert/glutathione.html

Tokuyasu, K.T. 1974. Dynamics of spermiogenesis in *Drosophila melanogaster* IV. nuclear transformation. *Journal of Ultrastructure Research* **48**: 284-303.

Tokuyasu, K.T. 1975. Dynamics of spermiogenesis in *Drosophila melanogaster* V. head-tail alignment. *Journal of Ultrastructure Research* **50**: 117-129.

Tokuyasu, K.T., Peacock, W.J., and Hardy, R.W. 1972. Dynamics of spermiogenesis in *Drosophila melanogaster* II. coiling process. *Zeitschrift fuer Zellforschung und Mikroskopische Anatomie* **127**: 492-525.

Toshimori, K., and Ito, C. 2003. Formation and organization of the mammalian sperm head. *Archives of Histology and Cytology* **66** (5): 383-396.

Valdez, J.M. 2001. Ultrastructure of the testis of the Mexican fruit fly (Diptera: Tephritidae). *Annals of the Entomological Society of America.* **94** (2): 251-256.

Vibranovski, M.D., Chalopin, D.S., Lopes, H.F., Long, M., and Karr, T.L. 2010. Direct evidence for postmeiotic transcription during *Drosophila melanogaster* spermatogenesis. *Genetics Society of America* **186**: 431-433.

Ward, W.S., and Coffey, D.S. 1991. DNA packaging and organization in mammalian spermatozoa: comparison with somatic cells. *Biology of Reproduction* **44**: 569-574.

White-Cooper, H. 2008. Studying how flies make sperm - investigating gene function in *Drosophila* testes. *Molecular and Cellular Endocrinology* doi: 10.1016/j.mce/2008.11.026.